

**Contrasting distributions and cycling of reduced sulfur compounds in saline and estuarine
waters of the coastal NE Subarctic Pacific**

by

Zhiyin Zheng

B.Sc., The University of British Columbia, 2019

A THESIS SUBMITTED IN PARTIAL FULFILLMENT OF
THE REQUIREMENTS FOR THE DEGREE OF

MASTER OF SCIENCE

in

THE FACULTY OF GRADUATE AND POSTDOCTORAL STUDIES

(Oceanography)

THE UNIVERSITY OF BRITISH COLUMBIA

(Vancouver)

July 2021

© Zhiyin Zheng, 2021

The following individuals certify that they have read, and recommend to the Faculty of Graduate and Postdoctoral Studies for acceptance, the thesis entitled:

Contrasting distributions and cycling of reduced sulfur compounds in saline and estuarine waters of the coastal NE Subarctic Pacific

submitted by Zhiyin Zheng in partial fulfillment of the requirements for

the degree of Master of Science

in Oceanography

Examining Committee:

Philippe Tortell, Professor, Department of Earth, Ocean, and Atmospheric Sciences, UBC
Supervisor

Kristin Orians, Professor, Department of Earth, Ocean, and Atmospheric Sciences, UBC
Supervisory Committee Member

Allan Bertram, Professor, Department of Chemistry, UBC
Supervisory Committee Member

Nadine Borduas-Dedekind, Professor, Department of Chemistry, UBC
Additional Examiner

Abstract

The trace gas dimethylsulfide (DMS) is considered to be one of the most important sulfur compounds in the marine environment. Research on this volatile sulfur compound has been stimulated by its potential role in regulating regional and global climate, and its importance, along with the related sulfur compounds, dimethylsulfoniopropionate (DMSP) and dimethylsulfoxide (DMSO), as carbon and sulfur sources for microbes in the marine environment.

The northeast subarctic Pacific (NESAP) is one of the global DMS hotspots, with significant spatial and temporal variability in DMS production. The difference in nutrient supply between coastal and offshore waters in this region drives significant variability in phytoplankton community structure, primary productivity, and thus sulfur cycling. The goal of this thesis is to characterize the patterns of sulfur cycling in two hydrographically distinct regimes in the NESAP, and to provide insights into the relative contribution of various DMS production pathways.

Chapter 2 presents new measurements of DMS, DMSP and DMSO (DMS/P/O) concentrations and turnover rate constants made in the coastal NESAP, as well as ancillary hydrographic and satellite data that help explain the underlying factors influencing DMS/P/O distributions and cycling. A strong linear relationship was demonstrated between DMS and DMSO concentrations, confirming similar ratios found in previous studies. Turnover rate constants for net DMS production from DMSO were comparable to those for DMSP, indicating DMSO reduction as an important pathway for marine DMS production. Similar rate constants for DMSP cleavage and DMSO reduction between the two regimes were found, although the lower average of $k_{\text{DMSPcleav}}$ in the continental shelf waters may indicate higher bacterial sulfur demand in the more productive shelf waters. Our findings provide insights into marine sulfur dynamics in adjacent but

contrasting marine waters, and highlight the significant contribution of DMSO to DMS production. This result suggests a need for improved understanding of marine DMSO cycling.

In addition to the main research presented in the body of this thesis, the Appendices present supplementary tests of various DMSP preservation methods, and a detailed protocol for DMSO reduction by the TiCl_3 method. These methodological details will be useful for future sulfur studies.

Lay Summary

The trace gas dimethylsulfide (DMS) and related sulfur compounds dimethylsulfoniopropionate (DMSP) and dimethylsulfoxide (DMSO) are integral parts of the marine sulfur cycle. They act as important food sources for marine bacteria, play several physiological functions in algal cells, and can also influence atmospheric chemistry and climate. This thesis examines the relative contribution of net DMS production from DMSP and DMSO, and compares the different sulfur cycles in the continental slope waters versus the shelf waters near the British Columbia coast. This research provides insights about the potential environmental drivers governing sulfur cycling in different marine waters, and highlights the significant contribution of DMSO to DMS production.

Preface

The work in this thesis was carried out using instrumentation and facilities provided by the Tortell Lab at the University of British Columbia. The data presented in Chapter 2 were collected using the OSSCAR underway system (Asher et al. 2015) and a custom-built proton-transfer mass spectrometer (McCulloch et al. 2020). Fieldwork and sample collection were conducted by me and Ross McCulloch. The OSSCAR underway system was initiated and developed by Elizabeth Asher, Philippe Tortell and John Dacey. Proton-transfer mass spectrometer used for tracer study was developed by Ross McCulloch. Ancillary samples were collected and analyzed by the Institute of Ocean Sciences. Data analysis, data interpretation and writing contained herein are my own, with significant guidance and contribution from Dr. Tortell. Dr. McCulloch also provided valuable feedback. A version of Chapter 2 is currently in preparation for submission to a scientific journal.

Table of Contents

Abstract	iii
Lay Summary.....	v
Preface	vi
Table of Contents.....	vii
List of Tables.....	x
List of Figures	xi
List of Abbreviations	xiii
Acknowledgements	xvi
Dedication.....	xviii
Chapter 1: Introduction.....	1
1.1 DMS Overview.....	1
1.2 Understanding of marine sulfur cycle to date.....	2
1.2.1 Physiological roles, sources and sinks of DMSP	2
1.2.2 Physiological roles, sources and sinks of DMSO.....	4
1.3 Current sulfur studies.....	5
1.3.1 Laboratory culture experiments.....	5
1.3.2 Field-based experiments.....	6
1.3.3 Limitation of existing sulfur studies.....	7
1.4 Thesis overview	8
Chapter 2: DMS production from DMSO reduction and DMSP cleavage in saline and estuarine waters of the coastal Subarctic NE Pacific	9

2.1	Introduction	9
2.2	Methods	13
2.2.1	Study area and hydrographic context	13
2.2.2	DMS/P/O Concentration measurements	15
2.2.3	Rate measurements	17
2.2.4	Ancillary measurements	20
2.2.5	Sea-air flux	21
2.2.6	Statistical analysis	22
2.3	Results	22
2.3.1	Oceanographic conditions	22
2.3.2	Underway DMS/P/O concentrations	23
2.3.3	Turnover rate constants	24
2.3.4	Sea-air flux	25
2.3.5	Comparison of distinct hydrographic domains	25
2.4	Discussion.....	27
2.4.1	DMS/P/O concentrations around Vancouver Island	27
2.4.2	DMS - DMSO Relationship	29
2.4.3	Sulfur cycling in slope and shelf waters.....	30
2.4.4	Comparison with previous rate measurements and methodological considerations	33
2.4.4.1	Comparison with rate measurements in the same area.....	33
2.4.4.2	Comparison with other tracer studies	34
2.4.4.3	Methodological considerations.....	34

2.4.4.4	DMS budget and mass balance.....	36
2.4.4.5	Implication of DMSO reduction in contribution to DMS production.....	37
2.4.4.6	Future studies.....	38
2.5	Conclusion.....	39
Chapter 3: Conclusion.....		52
3.1	Major findings.....	52
3.2	Limitations and future outlook.....	53
Bibliography.....		55
Appendices.....		69
Appendix A DMSP preservation.....		69
A.1	Optimal amount of acid used for preservation.....	70
A.2	Acidification method.....	70
A.3	Microwave method.....	72
Appendix B Protocol of DMSO analysis by $TiCl_3$		73
B.1	Preparation of glassware prior to analysis.....	73
B.2	Experimental procedures of DMSO reduction by $TiCl_3$	74
Appendix C Supplementary materials for Chapter 2.....		75
C.1	Calculation of turnover rate constants for net DMS production from DMSP cleavage and DMSO reduction.....	75
C.2	Statistical assessment of turnover rate constants.....	77
C.3	Supplementary figures for discussion.....	79

List of Tables

Table 2.1 Summary of Chl <i>a</i> concentrations, total DMS/P/O concentrations and rate constants from 20 incubation stations. Error bars represent one standard error.	40
Table 2.2 Estimated DMS budget from biological production/consumption rates. Rates for DMSP _d cleavage are calculated by estimating $DMSP_d : DMSP_t = 3.64\%$ from Royer et al., (2010). Error bars represent one standard error.....	41

List of Figures

Figure 2.1 Ship track (black lines) and location of tracer experiments (white circles) from La Perouse cruise in September, 2019. WCVI, QCS and SoG denote West Coast of Vancouver Island, Queen Charlotte Sound and Strait of Georgia, respectively. Colormap represents bathymetry. The light grey solid line represents the 200m isobath.....	43
Figure 2.2 Distributions of (a) sea surface temperature (SST); (b) salinity; (c) mixed layer depths (MLD); and relative abundance of diatoms (d), dinoflagellates (e), and prymnesiophytes (f) derived from HPLC-based pigment analysis during the September, 2019 cruise. Grey solid lines represent the 200 m isobath.....	44
Figure 2.3 Comparison of discrete in-situ Chl <i>a</i> measurements (colored dots) and satellite-based Chl <i>a</i> measurements (background color) derived from the 8-day MODIS-Aqua satellite averaged from Aug 21-Sep 13, 2019. Colorbar scale is logarithmic. The grey solid line represents the 200 m isobath. The figure demonstrated good coherence between satellite and discrete Chl <i>a</i> data...	45
Figure 2.4 Concentrations of surface water (a) DMS, (b) DMSP and (c) DMSO around Vancouver Island in September, 2019. Round scatter points (●) are underway measurements from the automated OSSCAR system; diamond scatter points (◆) are discrete samples analyzed in the laboratory. Measurements for DMSP and DMSO are not available from the early cruise samples due to instrument problems.	46
Figure 2.5 Linear relationship between DMS and DMSO concentrations around Vancouver Island during September, 2019. The black dashed line represents a linear fit to the data ($DMSO_t = 0.42 \times DMS + 0.79, r = 0.81, p \ll 0.001$). The dashed-dot line indicates the linear	

fit to the May, 2017 data obtained by Herr et al. (2020) ($DMS_{0t} = 0.92 \times DMS + 0.47$, $r = 0.77$, $p \ll 0.001$), and the black dotted line indicates a 1:1 relationship.47

Figure 2.6 Rate measurements of (a) net DMS change, (b) gross DMS consumption, (c) DMS production from DMSP cleavage, and (d) DMS production from DMSO reduction. Rate constants below detection limit are shown as hollow symbols (\diamond). The grey solid line in each panel represents the 200 m isobath.48

Figure 2.7 Ship-track distribution of (a) DMS/P/O concentrations; (b) sea surface salinity, temperature and discrete Chl *a* samples; (c) relative abundance of diatoms, dinoflagellates and haptophytes; and (d) turnover rate constants of DMSP cleavage and DMSO reduction. Note that the rate constant for DMSO reduction at station SS5 ($k = 0.29 \pm 0.02 \text{ d}^{-1}$) exceeds the y-scale, and is not plotted. Grey patches indicate the QCS region. Error bars represent one standard error.49

Figure 2.8 (a): Results from PCA and k-mean clustering analysis using Chl *a*, NO_3 , PO_4 , Si, salinity, temperature, density, MLD and relative abundance of different phytoplankton groups as input variables. The first two PC axes explain 67% of total variance of the dataset. Diamonds and circles represent two clustering ($k = 2$) groups; white diamond symbols in dark blue represent slope stations, and black round symbols in light blue represent on-shelf stations. (b): Locations of discrete incubation stations superimposed on the sea surface height anomaly derived from remote sensing observations. Grey solid line represents the 200 m isobath.50

Figure 2.9 Comparison of various environmental variables, sulfur concentrations and rate constants between the slope and on-shelf stations. Variables with statistical differences between the two sets of stations are marked with a red asterisk. Error bars indicate one standard error.51

List of Abbreviations

CCN: cloud condensation nuclei

Chl *a*: Chlorophyll-*a* pigment

CTD: oceanographic instrument to measure conductivity, temperature and depth of seawater

DMS: dimethylsulfide

D₃-DMS: isotopically labelled dimethylsulfide with three deuterium atoms on one methyl group

D₆-¹³C₂-DMSO: isotopically labelled dimethylsulfoxide with three deuterium atoms on both methyl groups and two carbons with atomic mass of 13

D₆-DMSP: isotopically labelled dimethylsulfoniopropionate with three deuterium atoms on both methyl groups

DMS/P/O: concentrations of dimethylsulfide, dimethylsulfoniopropionate and dimethylsulfoxide

DMSO: dimethylsulfoxide

DMSO₂: dimethylsulfone

DMSO_d: dissolved dimethylsulfoxide

DMSO_p: particulate dimethylsulfoxide

DMSO_t: total dimethylsulfoxide

DMSOP: dimethylsulfoxonium

DMSOr: dimethylsulfoxide reductase

DMSP: dimethylsulfoniopropionate

DMSP_d: dissolved dimethylsulfoniopropionate

DMSP_p: particulate dimethylsulfoniopropionate

DMSP_t: total dimethylsulfoniopropionate (particulate + dissolved)

FRRF: fast repetition rate fluorometer

F_v/F_m: a measurement ratio that represents photochemical efficiency of photosystem II

HPLC: high performance liquid chromatography

k: reaction rate constant

L: liter

LED: light-emitting diode

MeSH: methanethiol

m/z: mass to charge ratio

MLD: mixed layer depth

NESAP: Northeast Subarctic Pacific

nM: nanomolar

NO₃: nitrate/nitrite concentrations

NPQ: non-photochemical quenching

·OH: hydroxyl radicals

OSSCAR: Organic Sulfur Sequential Chemical Analysis Robot

PAR: photosynthetically active radiation

PCA: principal component analysis

PFPD: pulsed-flame photometric detector

PO₄: phosphate concentrations

QCS: Queen Charlotte Sound

ROS: reactive oxygen species

SSHA: sea surface height anomalies

Si: silicate concentrations

SoG: Strait of Georgia

SST: sea surface temperature

TiCl₃: titanium chloride

VICC: Vancouver Island Coastal Current

WCVI: west coast of Vancouver Island

Acknowledgements

I have been feeling fortunate, thankful and grateful to meet many amazing people who have introduced me into, guided me through, and supported me throughout the journey of oceanographic research. First and foremost, I would like to thank my supervisor, Dr. Philippe Tortell, for offering me the opportunity into the world of oceanography while I was an undergraduate who knew nothing about ocean. Thank you for your guidance and support throughout this project, and for revising my 30+ pages of manuscript at 4am in the morning. I feel extremely fortunate, indeed, to have you as my first supervisor in my early career. I learned a lot from you, from many aspects. I would also like to thank Dr. Cara Manning, for being my first mentor in oceanographic research, and for whispering what CTD stands for at my very first lab meeting in an oceanography group. Thank you for spending the time on Friday afternoon troubleshooting instruments together, and for sharing the most incredible Arctic glacial view on our way to the rosette room at 3am. To Dr. Ross McColloch, for all of the inspiring conversations about research and life. Thank you for being so supportive, always, the whole time, thank you. Thanks to Dr. Kristin Orians and Dr. Allan Bertram for their valuable inputs to this thesis.

I am indebted for the friendship from my colleagues. Thank you, Robert, for the jokes, laughs, chats, distractions, and for sharing sunset from the window of Room 2041 in many winter afternoons. Thank you, Florian, for the good time in Room 2041 we spent together in pre-covid era, and for sharing your passion about jellyfish. Thank you, Alysia, for setting up the OSSCAR on my La Perouse cruise and always answering my endless questions. Thank you Tortellinis-Brandon, Kate, Yayla, Chen, Chuan, Sarah, Ana- I wish we could spend more good time together if there was no pandemic. Thanks to the Saanich team, Julia, Chris, Sachia, Jade, Grace, for the

science fun from sunny to stormy days. Thanks to many wonderful people I met at UBC, Nick, Cheng, Yuanji, Iselle, Lori, Wylee, Mina, David.

Many thanks to the captains and crews of the CCGS *John P Tully*, who made this work possible at sea. Thanks to Akash Sastri and Ian Perry, for your support and conversations during the cruise. Thanks to Nina Nemcek and Angelica Peña for providing Chlorophyll a and HPLC pigment data.

Finally, I would like to express my appreciation to my friends and family. Thanks to my friends for taking me out for hikes, food and good company. A special and deepest thank you to my parents; to my mom, for always supporting me in the warmest and sweetest way; to my dad, for leading me, guiding me, and loving me since day zero and till forever.

致爸爸，妈妈，和妹妹

Chapter 1: Introduction

1.1 DMS Overview

The marine biogenic trace gas dimethylsulfide (DMS), produced by marine phytoplankton and bacterioplankton, is an integral part of the marine sulfur cycle (Kiene and Linn 2000). DMS has received extensive research attention for more than 40 years due to its potential role in regulating regional and global climate (Lovelock et al. 1972; Charlson et al. 1987). Several decades ago, Charlson et al. (1987) proposed a famous CLAW hypothesis, which suggested a DMS-mediated feedback loop between marine DMS emission and atmosphere. After being ventilated into the atmosphere, DMS is rapidly oxidized to form sulfate aerosols, which act as cloud condensation nuclei (CCN). Increased CCN enhances cloud albedo, leading to greater backscattering of incoming solar radiation. Hence, the oceanic flux of DMS in the atmosphere may potentially offset the warming effect by increased CO₂ emissions. Furthermore, cloud formation would decrease both irradiance levels and UV exposure to phytoplankton, thus potentially altering biological productivity in marine surface waters.

Recent research has challenged the connection between oceanic DMS emissions and CCN, and hence the proposed climate regulation role of marine DMS (Vallina et al. 2007; Quinn and Bates 2011). Those authors argue that non-DMS-derived particles may act as the dominant CCN, and field measurements revealed S-contained gases coagulated with sea salts and organics for formation of CCN (Murphy et al. 1998). Those results suggest that DMS itself is less likely to serve as CCN, especially in areas with greater aerosol contribution from anthropogenic emissions.

Irrespective of its potential climate influence, surface ocean DMS and the related sulfur compounds, dimethylsulfoniopropionate (DMSP) and dimethylsulfoxide (DMSO), serve as

important substrates and carbon and sulfur sources to marine microbial food web (Kiene and Linn 2000; Kiene et al. 2000; Simó 2001; Hatton et al. 2004; Vila-Costa et al. 2006b; Stefels et al. 2007). In phytoplankton cells, these three reduced sulfur compounds have been suggested to play several physiological roles, such as cryoprotection, osmo-regulation, and anti-oxidant function (Kiene et al. 2000; Stefels 2000; Sunda et al. 2002; Hatton et al. 2004). In general, the multifaceted ecological and biogeochemical roles of DMS/P/O continue to interest atmospheric scientists and oceanographers. In the following section, physiological functions, and sources and sinks of those marine sulfur compounds will be discussed in detail.

1.2 Understanding of marine sulfur cycle to date

1.2.1 Physiological roles, sources and sinks of DMSP

DMSP, an algal precursor of DMS, is synthesized in a broad spectrum of phytoplankton species, mainly those in several taxonomic groups, including Haptophyceae (Prymnesiophyceae) and Dinophyceae, as well as some members of Bacillariophyceae (diatoms) (Simó 2001; Stefels et al. 2007). Studies have demonstrated several physiological roles of algal DMSP, including osmoprotection and cryoprotection (Nishiguchi and Somero 1992; Stefels 2000), and scavenging of reactive oxygen species (ROS) under conditions of nutrient limitation and/or excess solar radiation (Sunda et al. 2002). In addition, an overflow mechanism of DMSP to dissipate excess energy and carbon under nutrient limitation is also hypothesized (Stefels 2000). When nitrogen (an essential element for amino acids) is limiting, phytoplankton cells continue to assimilate sulfur and synthesize DMSP without incorporating amino acids into proteins (Stefels 2000; Bullock et al. 2017). Notably, recent studies have detected DMSP biosynthesis in some marine bacteria (Curson et al. 2017; Williams et al. 2019). Those authors proposed that bacterial DMSP synthesis

is upregulated by salinity, nutrient and temperature stressors, indicating similar physiological functions of DMSP in heterotrophic bacteria.

There are several consumption pathways of cellular DMSP by phytoplankton. Some DMSP-producing phytoplankton species can directly cleave cellular DMSP via the enzyme DMSP-lyase, thus liberating DMS (and acrylate) for intracellular metabolic use or excretion (Stefels 2000; Stefels et al. 2007). Cellular DMSP in particulate form (DMSP_p) can also be released into the dissolved seawater pool through exudation, cell lysis or zooplankton grazing (Stefels et al. 2007; Archer et al. 2011). In the dissolved pool, DMSP (DMSP_d) is consumed by bacteria via two pathways. The assimilatory demethylation/demethiolation pathway produces methanethiol (MeSH) as a carbon and reduced sulfur source for bacterial metabolism at a lower energetic cost (Simó 2001). The DMSP cleavage pathway generates acrylate as a carbon source and the less readily used DMS (Kiene et al. 2000; Stefels 2000; Sunda et al. 2002). Numerous laboratory and field studies have demonstrated that the demethylation/demethiolation pathway dominates under most natural conditions, and that the relative contribution of DMSP converted to DMS depends on bacterial growth rates and sulfur demands (Kiene and Linn 2000; Kiene et al. 2000; Stefels et al. 2007; Tripp et al. 2008). Field studies also show that the genes responsible for demethylation are expressed at higher levels in surface marine waters than those for DMSP cleavage, suggesting a preferential process of demethylation in the surface (e.g., Zheng et al. 2020).

More recently, Barak-Gavish et al. (2018) proposed DMSP as a mediator of bacterial virulence through various cellular pathways. They found that the amino acids produced from the DMSP demethylation pathway may act as precursors for the synthesis of bacterial algicides, thus leading to cell death. These authors also suggested that DMSP act as a chemotaxis cue, enabling bacteria to locate and physically attach to algal cells, as a precursor to infection.

1.2.2 Physiological roles, sources and sinks of DMSO

In contrast to the in-depth understanding of the ecological and biogeochemical dynamics of DMS and DMSP, less is known about DMSO as an integrated component of the marine sulfur cycle. This molecule has been hypothesized to play several physiological roles in phytoplankton, including cryoprotection, hydroxyl radical scavenging, and intracellular electrolyte balance (Lee and de Mora 1999). Sunda et al. (2002) also suggested that DMSO contributes to the cellular oxidative stress defense mechanism, due to its ability to scavenge ROS such as hydroxyl radicals ($\cdot\text{OH}$). More recently, Spiese and Tatarkov (2014) have shown that DMSO reduction activity (DRA) increases in response to nutrient limiting conditions, further suggesting that DMSO plays a role in algal stress responses.

DMSO is believed to be produced primarily from the biological (mediated by phytoplankton or bacteria) and photochemical oxidation of DMS (del Valle et al. 2007, 2009; Spiese et al. 2009), although the relative contribution of these processes likely varies between coastal and open ocean environments (Hatton 2002; Yang et al. 2007). In contrast, DMSO reduction to DMS appears to be dominated by biological processes (mediated by phytoplankton or bacteria), with DRA ubiquitous in all marine phytoplankton species examined to date, including those without DMSP-lyase activity (Stefels et al. 2007; Spiese et al. 2009). Therefore, the biological conversion between DMS and DMSO (either within phytoplankton cells or in the water column) is a two-way reaction. Particulate DMSO (DMSO_p), which has a high membrane permeability, is lost via diffusion across the cell membrane into the surrounding water column (Tanaka et al. 2001). Other removal pathways of cellular and dissolved DMSO (DMSO_d) include

assimilatory and dissimilatory use, oxidation to dimethylsulfone, and export out of the water column in sinking particles (Hatton et al. 2004).

Compared to DMSP, the mechanisms linking DMSO to other parts of the marine sulfur cycle remain poorly identified. Recently, Thume et al. (2018) discovered a new metabolite in the sulfur cycle, dimethylsulfoxonium propionate (DMSOP), which is synthesized by DMSP-producing phytoplankton and some marine bacteria. Results from this work demonstrated that DMSOP is produced from DMSP via a direct oxidative production pathway by marine phytoplankton or bacteria. It was also suggested that bacterioplankton are able to further degrade DMSOP to DMSO. This reveals a previously undescribed pathway for marine DMSO production, in addition to DMS oxidation.

1.3 Current sulfur studies

1.3.1 Laboratory culture experiments

In recent years, many studies have investigated the physiological roles of DMS/P/O and biogeochemical dynamics of the marine sulfur cycle, both in the laboratory and in the field. Controlled experiments with laboratory batch cultures have been conducted to understand the environmental constraints and drivers (e.g., nutrients, temperature, and salinity) of the sulfur compounds and their proposed physiological roles (e.g., antioxidants and osmo-protectants). To examine the hypothesized antioxidant function of DMSO, Spiess and Tatarkov (2014) studied the response of DRA to nutrient limitation in cultured marine diatoms. Their study revealed that cellular DMSO and DRA increased during nutrient limiting conditions, suggesting a physiological role in nutrient stress management for DMSO and DRA. To understand the response of these sulfur compounds to other oxidative stressors, Speeckaert et al. (2019) investigated the effects of salinity

and growth phases on cellular DMSP and DMSO in phytoplankton. They suggested that DMSP acts as an osmo-regulator in response to salinity change, while DMSO acts as an antioxidant under oxidative stress. Similarly, Wittek et al. (2020) also investigated the proposed metabolic functions of DMSP and DMSO as an osmo-regulator and cryoprotectant by quantifying the cell quotas of DMSP and DMSO in the sea-ice diatoms under a gradient of salinity and temperature. Their results suggested that these two compounds serve as osmo-regulators under higher salinity conditions. No significant temperature-dependent changes in DMSP and DMSO cell quotas were observed, indicating that the cryoprotection functions of DMSP and DMSO may not be relevant in these Antarctic diatoms.

1.3.2 Field-based experiments

In contrast to controlled laboratory experiments, where phytoplankton cultures are grown under controlled and axenic conditions, field-based experiments have also been performed to understand the complexity of the biogeochemistry of marine sulfur cycle. In general, there are two types of field-based studies: concentration measurements to investigate the spatial and temporal variability of sulfur compounds, and turnover rate experiments to examine the relative contribution of various pathways to DMS production.

As an example of recent concentration measurements, Speeckaert et al. (2018) measured the annual cycle of the *in-situ* DMS, DMSP and DMSO concentrations to understand the relationship between these sulfur compounds and phytoplankton succession. Their results revealed strong seasonal variations in DMS/P/O concentrations associated with phytoplankton species succession throughout the year, yielding two different relationships between DMSP and chlorophyll a (Chl *a*) concentrations. In addition to seasonal variability, other studies have

examined diurnal changes in DMS/P/O, in relation to photo-chemical processes (i.e., DMS photo-oxidation to DMSO). Zhou et al. (2020) observed obvious diurnal variations of DMSO_d and DMS, suggesting photo-oxidation and biological oxidation of DMS may be important sources of DMSO_d. Similarly, Herr et al. (2020) investigated DMSO diel cycling in the Lagrangian drift survey. In their study, DMSO concentrations were strongly coupled with non-photochemical quenching (NPQ) and the photochemical efficiency of photo-system II (Fv/Fm), suggesting a photo-protective role of DMSO.

Field-based incubation experiments have been conducted to measure the turnover rates and biological consumption of DMS/P/O. For example, Li et al. (2015) used stable isotope tracers to study the turnover of dissolved DMSP in coastal water samples, providing the first evidence of a refractory DMSP_d pool that is resistant to degradation by the heterotrophic bacterial community. More recently, Tyssebotn et al. (2017) studied the bacterial uptake of DMSO using dark incubations that eliminated photochemical processes. Their results suggested a slow turnover time of DMSO_d (days), and demonstrated that the majority of DMSO was respired by the microbial community, thereby calling into question the relative contribution of DMSO_d reduction to DMS production in comparison to other removal pathways (e.g., respiration, oxidation to dimethylsulfone).

1.3.3 Limitation of existing sulfur studies

Although there have been numerous studies on DMS production from DMSP, and recent information on the mechanisms linking marine DMS and DMSO, very few studies have simultaneously compared *in-situ* DMSP cleavage to DMS and DMSO reduction to DMS (Asher et al. 2011a, 2017a; b; Dixon et al. 2020; Herr et al. 2020). Results from isotope tracer experiments

have demonstrated comparable DMS production rates from DMSP cleavage and DMSO reduction (Asher et al. 2017a), and, in some cases, DMSO reduction rate exceeding those of DMSP cleavage (Asher et al. 2011a, 2017b). These results suggest that DMSO plays a potentially significant, and previously under-appreciated, role in marine DMS production. However, given the scarcity of *in-situ* turnover rate measurements of a variety of sulfur transformations, more field sampling is required to better understand the importance of these different pathways across various hydrographic regimes.

1.4 Thesis overview

In this study, we build on the recent work of Asher et al. (2011, 2017a; b) and Herr et al. (2019, 2020), examining the rates of DMS production via DMSP cleavage and DMSO reduction in the Subarctic Pacific Ocean, a global DMS production hotspot (Lana et al. 2011). We conducted ship-based field work combining high-resolution, underway measurements of surface water DMS/P/O concentrations, and stable isotope tracer experiments to quantify turnover rate constants for DMS/P/O conversions. Our new field observations provide insights into the spatial and temporal dynamics of different DMS production pathways, identifying distinct patterns across different near-shore hydrographic regimes, including the West Coast of Vancouver Island (WCVI), Queen Charlotte Sound (QCS), and the estuarine surface waters of the Strait of Georgia (SoG).

Chapter 2: DMS production from DMSO reduction and DMSP cleavage in saline and estuarine waters of the coastal Subarctic NE Pacific

2.1 Introduction

For more than 40 years, the marine biogenic trace gas dimethylsulfide (DMS) has received significant research attention due to its potential role in regulating regional and global climate (Lovelock et al. 1972; Charlson et al. 1987), and as an integral part of the marine sulfur cycle (Kiene and Linn 2000). After being ventilated into the atmosphere, DMS is rapidly oxidized to form sulfate aerosols, which act as cloud condensation nuclei (CCN). Increased CCN enhance cloud albedo, leading to greater reflection and back-scattering of incoming solar radiation (Charlson et al. 1987). Charlson et al. (1987) proposed that the resulting negative radiative forcing may, in turn, affect marine biological activity and DMS emissions, leading to a DMS-mediated feedback loop. Although recent research has challenged the connection between oceanic DMS emissions, CCN and climate regulation (Vallina et al. 2007; Quinn and Bates 2011), the multifaceted ecological and biogeochemical roles of this volatile organic compound and related marine sulfur compounds (Kiene et al. 2000; Stefels 2000; Sunda et al. 2002; Hatton et al. 2004) continue to interest atmospheric scientists and oceanographers.

DMS is produced as a degradation product of dimethylsulfoniopropionate (DMSP), which is synthesized by a broad spectrum of marine phytoplankton and bacteria, and serves multiple physiological roles (Simó 2001), including osmoprotection and cryoprotection (Nishiguchi and Somero 1992; Stefels 2000), and scavenging of reactive oxygen species under conditions of nutrient limitation and/or excess solar radiation (Sunda et al. 2002). Some DMSP-producing

phytoplankton species can directly cleave cellular DMSP via the enzyme DMSP-lyase, thus liberating DMS (and acrylate) for intracellular metabolic use or excretion (Stefels 2000; Stefels et al. 2007). Intracellular DMSP exists in the particulate phase (DMSP_p), but can also be released into the dissolved seawater pool through exudation, cell lysis or zooplankton grazing (Stefels et al. 2007; Archer et al. 2011). Dissolved DMSP in seawater (DMSP_d) is an important organic carbon and sulfur source for bacteria (Kiene and Linn 2000; Kiene et al. 2000; Simó 2001), and is consumed via two pathways; the assimilatory demethylation/demethiolation pathway, which produces methanethiol (MeSH) as a metabolic carbon and reduced sulfur source; and the DMSP cleavage pathway, which generates acrylate as a carbon source and the less readily used DMS (Kiene et al. 2000; Stefels 2000; Sunda et al. 2002). Numerous laboratory and field studies have demonstrated that the demethylation/demethiolation pathway dominates under most natural conditions, with the relative DMS yield from DMSP depending on bacterial growth rate and sulfur demand (Kiene and Linn 2000; Kiene et al. 2000; Stefels et al. 2007; Tripp et al. 2008). Across a variety of oceanic systems, DMS yields have been reported to range from <1 to >400 nM. Recently, Barak-Gavish et al (2018) proposed DMSP as a mediator of bacterial virulence through various cellular pathways, including the production of amino acid precursors for the synthesis of bacterial algicides, and as a chemotaxis cue enabling bacteria to locate and attach to algal cells, resulting in algicidal activity.

DMS can also be produced from another sulfur compound, dimethylsulfoxide (DMSO), via biological DMSO reduction (Hatton et al. 2004). In comparison to DMS and DMSP, less is known about the ecological and biogeochemical roles of DMSO in the marine sulfur cycle. This molecule has been suggested to play several physiological roles in phytoplankton, including cryoprotection, hydroxyl radical ($\cdot\text{OH}$) scavenging, and intracellular electrolyte balance (Lee and

de Mora 1999). Sunda et al. (2002) have also suggested that DMSO may serve to mitigate cellular oxidative stress due to its ability to scavenge reactive oxygen species (ROS).

Production and consumption pathways of DMSO have been investigated in recent years. DMSO is believed to be produced primarily from the biological and photochemical oxidation of DMS (del Valle et al. 2007, 2009; Spiese et al. 2009), although the relative contribution of these processes may vary between coastal and open ocean environments (Hatton 2002; Yang et al. 2007). Recently, Thume et al. (2018) have identified an alternate DMSO production pathway from the bacterial degradation of dimethylsulfoxonium propionate (DMSOP), a metabolite synthesized by DMSP-producing phytoplankton and some marine bacteria.

Among the various DMSO removal pathways, DMSO reduction is of particular interest. This process appears to be primarily biological (mediated by both phytoplankton and bacteria), with DMSO reduction activity (DRA) ubiquitous in all marine phytoplankton species examined to date, including those without DMSP-lyase activity (Stefels et al. 2007; Spiese et al. 2009). DMSO reduction has been shown to increase in response to nutrient limitation, suggesting that DMSO plays a role in algal stress response (Spiese and Tatarkov 2014). In addition to biological reduction, DMSO produced within phytoplankton cells is suggested to function as part of the DMS-DMSP-DMSO antioxidant cycle (Sunda et al. 2002; Spiese et al. 2009). It can also diffuse into the surrounding seawater due to its high membrane permeability (Tanaka et al. 2001). Spiese et al. (2009) suggested that cellular DMS oxidation to DMSO potentially serves as a signal of oxidative stress, triggering the transcription of genes responsible for DMSO reduction to regenerate DMS. In this way, biological oxidation and reduction reactions may drive a rapid two-way interconversion between DMS and DMSO. Other removal pathways of cellular and dissolved

DMSO (DMSO_d) include assimilatory and dissimilatory use, oxidation to dimethylsulfone (DMSO_2), and export from the water column by sinking particles (Hatton et al. 2004).

Although there have been numerous studies of DMS production from DMSP, and more recent work examining mechanisms linking marine DMS and DMSO (Hatton et al. 2012; Lidbury et al. 2016), few studies have simultaneously measured and compared *in situ* DMS production from DMSP cleavage and DMSO production (Asher et al. 2011a, 2017a; b; Herr et al. 2020). Results from stable isotope tracer experiments have demonstrated comparable DMS net production rates from DMSP cleavage and DMSO reduction in the dissolved pool (Asher et al. 2017a), with DMSO reduction rate sometimes exceeding those of DMSP (Asher et al. 2011a, 2017b; Herr et al. 2020). These results suggest that DMSO may play a potentially significant, and previously under-appreciated role in marine DMS production.

In this study, we build on the recent work of Asher et al. (2011, 2017a; b) and Herr et al. (2019, 2020) examining turnover rate constants of DMSP and DMSO pathways in the coastal NESAP, a global DMS production hotspot (Lana et al. 2011). Our study area covered two hydrographically distinct regions within the waters surrounding Vancouver Island, from the river-influenced continental shelf region to more saline waters over the continental slope. These distinct regions are influenced by various physical processes driven by environmental conditions, including riverine input, coastal upwelling, tidal mixing and estuarine circulation (Ianson et al. 2003; Whitney et al. 2005). This physical variability, in turn, drives regional patterns in nutrient delivery and phytoplankton dynamics (Boyd and Harrison 1999; Peterson et al. 2007; Harris et al. 2009), but it is presently unclear how this may affect regional sulfur cycling. To address this question, we conducted high-resolution, ship-board measurements of surface water concentrations of DMS, DMSP and DMSO (DMS/P/O) along the British Columbia coastal region, coupled with

stable isotope tracer experiments to quantify turnover rate constants for DMS/P/O inter-conversion. Our observations compare DMS/P/O concentrations and turnover rates in two distinct hydrographic regimes and examine potential drivers of sulfur dynamics. We also discuss the caveats and limitations of current tracer studies, and suggest avenues for future work.

2.2 Methods

2.2.1 Study area and hydrographic context

Field sampling in the NE Pacific Ocean was conducted on board the *CCGS John P. Tully* during late summer, 2019. We surveyed the coastal waters adjacent to Vancouver Island, including the west coast of Vancouver Island (WCVI), Queen Charlotte Sound (QCS) and the Strait of Georgia (SoG), British Columbia, Canada (Fig. 2.1). Data were collected between 29th August and 9th September, as part of the La Perouse program run by Fisheries and Oceans Canada.

The regional oceanography of our study area is influenced by the seasonal timing of summer upwelling and winter downwelling, and freshwater discharge from the Fraser River (Bylhouwer et al. 2013; Jackson et al. 2015). Off the WCVI, upwelling primarily occurs in summer (Apr-Sept), transporting nutrient-rich deep waters onto the shelf, whereas downwelling conditions dominate in fall and winter (Oct-Mar) (Thomson 1981; Ianson et al. 2003; Jackson et al. 2015). In addition, the Vancouver Island Coastal Current (VICC) is a year-round buoyancy-driven flow running from the entrance of Juan de Fuca Strait to north of Brooks Peninsula along the inner shore of WCVI (Freeland et al. 1984; Hickey et al. 1991; Ianson et al. 2003; Harris et al. 2009; Jackson et al. 2015). This surface coastal current supplies relatively low salinity water and nutrients from Juan de Fuca Strait, and supports elevated summertime productivity along the southern Vancouver

Island coast and inner continental shelf off the WCVI (Freeland et al. 1984). Along the outer shelf, a southeastward flowing Shelf-Break Current dominates in the surface layer during summer (Freeland et al. 1984; Jackson et al. 2015). Nanoflagellates are the dominant phytoplankton group in both the offshore and nearshore regions, with the contribution of diatoms increasing over the continental shelf, particularly during summer months (Harris et al. 2009).

In the QCS region, surface water nutrients are typically supplied by summer upwelling (Peterson et al. 2007; Jackson et al. 2015) and fresh water outflow from Rivers Inlet (Whitney et al. 2005). In addition, anticyclonic Haida eddies, formed near the southern tip of Haida Gwaii in winter, propagate westward, supplying nutrients (including iron and silicate) into surface waters off the west coast of Haida Gwaii and adjacent oceanic waters (Crawford 2002; Whitney and Robert 2002; Keith Johnson et al. 2005). Satellite images reveal enhanced chlorophyll *a* around the perimeter of Haida eddies (e.g. Whitney et al. 2005). The dominant phytoplankton groups in the QCS region are typically diatoms and dinoflagellates, although the abundances of these groups exhibit strong temporal and spatial variability (Peterson et al. 2007, 2011).

Surface water in the SoG is strongly impacted by tidal mixing and freshwater input from the Fraser River, which peaks during the summer freshet (Thomson 1981; Masson and Pena 2009). Summertime temperatures in the SoG are typically warmer than in Johnstone Strait due to strong stratification (Thomson 1981; Tortell et al. 2012). The timing of the diatom-dominated spring bloom in the SoG varies from February to April, depending on biotic and abiotic conditions including solar radiation, temperature and grazing (Stockner et al. 1979; Harrison et al. 1983). Following the spring bloom, phytoplankton communities in the SoG are characterized by smaller-sized groups, such as prasinophytes and cryptophytes (Harrison et al. 1983; Del Bel Belluz et al. 2021).

2.2.2 DMS/P/O Concentration measurements

Concentrations of DMS, total (i.e. dissolved plus particulate) DMSO (DMSO_t) and total DMSP (DMSP_t) in surface water were measured using the previously described Organic Sulfur Sequential Chemical Analysis Robot (OSSCAR; Asher et al. 2015). This analytical system has been deployed on several previous cruises (Asher et al. 2015; Jarníková et al. 2018; Herr et al. 2019, 2020), and only a brief overview is given below. The reader is referred to Asher et al. (2015) for a full description of the instrument.

The system consists of a custom-built sample handling module for underway seawater collection and chemical reactions of DMSO and DMSP, a purge-and-trap and gas chromatography system to extract and separate DMS from other volatile gases, and a pulsed-flame photometric detector (PFPD). Seawater is drawn from the ship's underway supply with an intake at ~7 m depth. 5 mL of unfiltered seawater is automatically dispensed into a sparging chamber for sequential analysis of DMS, DMSO and DMSP. For DMS analysis, ultra-high purity (99.999%) N₂ is bubbled through the sample (~100 ml/min) to strip dissolved DMS out of the sample and onto a room temperature stainless-steel thermal desorption trap (Markes International, C3-AXXX-5266). Rapid electrical heating of the trap results in analyte desorption, and the resulting gas mixture is delivered onto a capillary column, where DMS is separated from other volatile compounds prior to detection by PFPD. Following DMS analysis, enzymatic conversion of DMSO to DMS is initiated by adding 2 mL of DMSO reductase (DMSOr) solution into the sparging chamber (Hatton et al. 1994). DMSO in the sample is enzymatically reduced to DMS under exposure to LED lights for 20 minutes, and the resulting DMS is measured using the purge-and-trap method described above. After DMSO analysis, 3 mL of 10N NaOH is added to the sparging chamber for DMSP

hydrolysis to DMS (Dacey and Blough 1987). The resulting DMS measured as outlined above. After the full DMS/P/O analysis sequence, the system completes a rinse cycle prior to the next sample analysis. The complete DMS/P/O cycle requires roughly 40 minutes. A 6-point calibration curve using DMS standard solutions is produced daily to check the system performance and for calculation of DMS/O/P concentrations.

In the absence of pre-filtering steps in our analysis, the concentrations of DMS/O/P reported here represent potential contributions from both the dissolved and particulate pools. For DMSP analysis, we assume that all phytoplankton cells were lysed by the addition of 10 M NaOH, such that DMSP concentrations measured by our system represent concentrations close to $DMSP_t$. However, the situation for DMSO analysis is more complex. The addition of DMSO_r into the sparging chamber is believed to act on the DMSO_d pool in the samples. However, due to the high cellular permeability of particulate DMSO (Tanaka et al. 2001), it is expected that particulate DMSO may diffuse into the surrounding seawater, increasing the apparent size of the DMSO_d pool. Herr et al. (2020) discuss the uncertainties of DMSO measurements by our system, pointing out that the LED lights used during the DMSO reduction step may enhance DMS production from DMSP due to oxidative stress, resulting in a potential overestimation of DMSO concentrations. In addition, the analytical sparging step in the analysis could potentially damage phytoplankton cells, releasing cellular DMSO into the dissolved pool. Therefore, the measured DMSO concentrations by our system likely represent DMSO concentrations closer to $DMSO_t$.

Discrete DMS/P/O samples were also collected at various stations across the sampling region. Approximately 10 L volume of seawater collected from a depth of 5 m was gently transferred into a 10 L carboy using flexible silicone tubing. Native DMS concentrations were obtained from the T0 samples of the tracer experiments (described in *Section 2.3*). Samples for

DMSP analysis were collected in 12 mL glass vials from the carboy using a spigot, and immediately preserved with 100 μ L of 25% H₂SO₄. Samples were sealed with rubber stoppers and crimped without headspace, before being immediately stored in the dark at 4 °C. Analysis of discrete DMSP samples was conducted in the laboratory, approximately 1 month after sample collection. Parallel DMSO samples were collected in similar 12 mL glass vials, which were filled halfway to accommodate volume expansion upon freezing. Samples were sealed with rubber stoppers and crimped without adding any preservative and stored at -80 °C prior to analysis. DMSO samples were analyzed approximately one year after sample collection using TiCl₃ method described by Kiene and Gerard (1994) and Deschaseaux et al. (2014).

2.2.3 Rate measurements

Using the stable isotope tracer method described by Asher et al. (2011, 2017a; b) and Herr et al. (2019, 2020), we measured rate constants of net DMS production, gross DMS consumption, and net DMS production from DMSP cleavage and DMSO reduction. This method enables simultaneous determination of rate constants for each of the four production/consumption pathways within a single incubation experiment. In September 2019, we conducted 20 tracer experiments in coastal waters of British Columbia, covering the WCVI, QCS, and SoG.

Seawater for rate measurements was collected in Niskin bottles from 5 m depth as described above in Section 2.2.2. The seawater in the 10 L carboy was spiked with isotopically labelled D₃-DMS (CDN Isotopes, 99.9% purity), D₆-DMSP (produced using the method in Challenger and Simpson 1948) and D₆, ¹³C₂-DMSO (ISOTECH, 99% purity) to obtain a final tracer concentration of ~1 nM. Spiked seawater was homogenized by gently inverting the carboy ~10 times, and 1L sub-samples were dispensed into triplicate UV-transparent FEP bags (Welch

Fluorocarbon). The bags were incubated in a deck-board seawater tank and maintained at *in situ* surface temperature by continuously flowing seawater. A plexiglass incubator lid was installed over the incubator, largely blocking UV exposure of incubation bags, thus minimizing any photochemical processes, such as the photo-oxidation of DMS to DMSO.

Incubation experiments were performed over a period of approximately 4 hours, during which 5 mL subsamples were collected every ~ 30 minutes from each incubation bag. DMS was analyzed in multiple reaction monitoring (MRM) mode using a Sciex (Concord, Ontario, Canada) API3200 triple quadrupole mass spectrometer, equipped with an atmospheric pressure chemical ionization source (McCulloch et al. 2020). In this method, DMS is ionized through a proton transfer mechanism, resulting in the formation of $[M+H]^+$ ions. Analyte ions are therefore measured at a mass to charge ratio (m/z) 1 unit higher than the native state. Concentrations of four isotopic species of DMS were measured over the course of the incubation period. Unlabeled DMS ($m/z = 63$) was monitored to track net DMS production, D_3 -DMS ($m/z = 66$) was used to estimate gross DMS consumption, D_6 -DMS ($m/z = 69$) was used to trace D_6 -DMSP cleavage and D_6 - $^{13}C_2$ -DMS ($m/z = 71$) was used to follow D_6 - $^{13}C_2$ -DMSO reduction. Rate constants for net DMS production and gross DMS consumption were calculated as pseudo-first order reactions by deriving the logarithmic slope concentration changes (natural logarithm of either m/z 63 or 66) from triplicate bags during the incubation period. Rate constants for net DMS production from biological DMSP cleavage and DMSO reduction were derived from a first order rate law (Uher et al. 2017), taking into account the initial concentrations of reactants (either D_6 -DMSP or D_6 - $^{13}C_2$ -DMSO) and products (D_6 -DMS or D_6 - $^{13}C_2$ -DMS)

$$\ln \left[\frac{C_0(D_6-DMSP) - \Delta C_t(D_6-DMS)}{C_0(D_6-DMSP)} \right] = -k_{DMSPcleav} \times t \quad \text{Eq. 1}$$

$$\ln \left[\frac{C_0(D_6-^{13}C_2-DMSO) - \Delta C_t(D_6-^{13}C_2-DMS)}{C_0(D_6-^{13}C_2-DMSO)} \right] = -k_{DMSOred} \times t \quad \text{Eq. 2}$$

where C_t and C_0 are concentrations at time t and $t = 0$, respectively; $\Delta C_t(D_6-DMS)$ and $\Delta C_t(D_6-^{13}C_2-DMS)$ are concentration change of isotopically labelled DMS derived from biological cleavage of D_6 -DMSP and biological reduction of D_6 - $^{13}C_2$ -DMSO, respectively. The resulting rate constants were expressed in units of day^{-1} .

Importantly, we note that the approach used here to derive rate constant calculations (equations 1 and 2) differs from that used by Asher et al. (2017a; b) and Herr et al. (2019, 2020). In these earlier studies, calculations were based only the rate of change of labelled products, without taking into account the starting concentration of labelled tracers. As documented in the appendices (Appendix C.1.1), these simplified calculations result in significantly higher derived rate constants. In our data set, for example, calculations using equations 1 or 2 produced rate constants more than 100-fold lower than those obtained from the calculations of Asher et al. (2017a; b) and Herr et al. (2019, 2020). In a re-analysis of the data from these earlier studies, we found a similar offset in derived rate constants. This discrepancy affects our comparison with absolute rate constants reported in earlier studies, but does not affect our conclusions regarding the relative rates of DMSP cleavage and DMSO reduction.

As per Asher et al. (2017a), incubation data producing regressions with $r^2 < 0.5$ were removed for calculation of rate constants. Detailed statistical criteria for removing outliers in the rate constant plots are discussed in the appendices (Appendix C.1.2). In total, this led to the

elimination of 1, 5, 3, and 2 out of 20 experiments of each sulfur transformations (net DMS change, gross DMS consumption, DMSP cleavage to DMS, and DMSO reduction to DMS).

2.2.4 Ancillary measurements

To characterize the oceanographic context of our study area, we obtained ancillary measurements from the shipboard underway sensors and at discrete sampling stations, as well as remote sensing data. Sea surface temperature and salinity were measured along the cruise track using a thermosalinograph (SeaBird 45 S/N 0620) at 5 m depth. For discrete sampling stations, a Sea-Bird CTD probe (SBE-911plus) equipped with a Wetlabs CSTAR transmissometer (#1883DG & 1185DR), a SBE 43 dissolved oxygen sensor (#3234), a SeaPoint Fluorometer (#3640), a Biospherical QSP-400 PAR sensor (#70613) and an altimeter was deployed for depth profile measurements of chlorophyll fluorescence, photosynthetically active radiation (PAR), salinity and dissolved oxygen. Mixed layer depth (MLD) at each CTD sampling station was calculated as the depth where density exceeded the surface values by 0.05 kg/m^3 . Discrete seawater samples of nitrate/nitrite (NO_3), phosphate (PO_4), silicate (Si), Chl *a*, and HPLC measurements for phytoplankton assemblage composition were collected and analyzed by the Institute of Ocean Sciences, following the methods of Barwell-Clarke and Whitney (1996) and Zapata et al. (2000). Ancillary measurements collected at 5 m depth were used for statistical analysis (described below). For some stations where 5 m measurements of Chl *a* and phytoplankton taxonomic composition were not available, surface samples (0 m) were used instead.

To provide a broader spatial and temporal context for our observations, we examined several remote sensing data products. Regional Chl *a* concentrations and PAR were derived from Level 3 8-day composite MODIS-Aqua satellite imagery at 4-km resolution

(<https://oceancolor.gsfc.nasa.gov/13/>). Chl *a* satellite data from Aug 21-Sep 13, 2019 were averaged to minimize cloud interference, while PAR data from Aug 28-Sep 4, 2019 were used. Monthly-averaged absorbance due to gelbstof and detritus at 443 nm was also obtained from the same satellite product, as a measure of chromophoric dissolved organic matter (CDOM) concentrations for photo-oxidation of DMS to DMSO (Nelson and Siegel 2013). Sea surface height anomalies (SSHA) were obtained and averaged from AVISO satellite altimetry using the Level 4 near real-time daily product with 0.25° resolution from Aug 29-Sep 9, 2019 (<https://las.aviso.altimetry.fr/las>).

2.2.5 Sea-air flux

The sea-air flux of surface DMS along the cruise track was calculated using OSSCAR underway DMS concentrations and the piston velocity derived from wind speeds, surface temperature and salinity:

$$F_{DMS} = k_w [DMS]_{aq}$$

where $[DMS]_{aq}$ is the surface concentration of DMS measured by the OSSCAR system, and k_w is the piston velocity based on parameterization by Sweeney et al. (2007). Following previous studies (e.g., Asher et al. 2017b; Herr et al. 2019), we assumed that atmospheric DMS concentrations are negligible for the purposes of sea-air flux calculations for DMS. Daily averaged wind speeds were derived from <http://www.remss.com/measurements/ccmp/>. Surface temperature and salinity were obtained from shipboard thermosalinograph data, as described above.

2.2.6 Statistical analysis

Linear regression analysis demonstrated a very limited number of statistically significant correlations between our sulfur measurements and environmental variables. As a result, we focused our analysis on the comparison of average values between different oceanographic sub-regions. Given the presence of various water masses within our study region, a principal component analysis (PCA) followed by a k-mean clustering analysis was applied to identify different hydrographically distinct regimes. Environmental parameters used in the PCA included Chl *a*, NO₃, PO₄, Si, salinity, temperature, density, MLD, dissolved oxygen, phaeo-pigment concentrations, and relative abundance of phytoplankton groups. For k-mean clustering, we found that $k = 2$ was the optimal clustering group number, as the sample size was relatively small ($n = 20$). A Mann-Whitney U test for non-parametric samples was performed to evaluate statistical differences among variables between the two regimes.

2.3 Results

2.3.1 Oceanographic conditions

Fig. 2.2 shows the distribution of surface water oceanographic properties across our study region, during September, 2019. At the time of our cruise, sea surface temperature and salinity ranged from 9.7 to 18.7 °C and from 21.0 to 32.6 psu, respectively. The warmest and most saline waters were observed along the west coast of WCVI and QCS (except for the eastern tip of QCS close to Rivers Inlet), whereas colder waters were mostly found in the Johnstone Strait and Juan de Fuca Strait due to strong tidal mixing processes. The more saline waters along the WCVI were indicative of their exposure to the Pacific Ocean, although a freshwater signature along the

southern WCVI was indicative of the near shore VICC. Maximum temperature (18.7 °C) and minimum salinity (21.0 psu) were observed in the surface waters of SoG, due to the Fraser River runoff which stratifies the near-surface waters during summer (Thomson 1981; Jackson et al. 2015). Mixed layer depths calculated from CTD profiles varied between 6.0 and 24 m. Shallower MLDs were observed along the eastern side of QCS and SoG, due to intensified stratification by river inputs (Rivers Inlet near QCS or Fraser River in the SoG).

The relative abundance of different phytoplankton groups across our study region exhibited typical distributions around Vancouver Island. Fig. 2.2 shows the relative abundance of diatoms, dinoflagellates and prymnesiophytes derived from HPLC-based pigment analysis. Diatoms were the most abundant species in the continental shelf waters around Vancouver Island, accounting for up to 90% of total Chl *a*. Dinoflagellates and prymnesiophytes dominated in the deeper slope waters of WCVI and QCS, contributing between 15% to 57% and <1% to 36% of total Chl *a*, respectively.

Fig. 2.3 compares the surface *in-situ* Chl *a* concentrations with satellite-derived values across our study area. *In-situ* Chl *a* concentrations ranged from 0.10-16 mg/m³, with maximum and minimum concentrations observed in inshore and offshore waters in the WCVI, respectively. Higher chlorophyll concentrations were present in the continental shelf waters of WCVI, QCS and SoG. In general, there was good coherence in the spatial distribution and absolute values of Chl *a* concentrations derived from ship-board analysis and remote sensing.

2.3.2 Underway DMS/P/O concentrations

Fig. 2.4 shows the DMS/P/O distributions along our cruise track. DMS concentrations in surface waters ranged from <0.1 to 31 nM, with a mean of 6.2 ± 0.5 nM. Due to instrument

problems at sea, underway DMSP and DMSO measurements are not available until the 5th day of our cruise (Sept. 2nd UTC time), and thus only underway DMS concentrations are shown for the southwestern portion of our WCVI transect.

The highest DMS concentrations (>20 nM) were observed in coastal waters of the La Perouse Bank and in QCS (Fig. 2.4). Total DMSP concentrations ranged from <2 to 528 nM (mean 103 ± 9 nM), with the maximum value (528 nM) observed in QCS. Total DMSO concentrations were comparable to DMS concentrations measured in our study, ranging from <0.1-15 nM (mean 3.6 ± 0.2 nM). Notably, DMSO concentrations exhibited a strong positive correlation with DMS concentrations ($r = 0.81$, $p \ll 0.001$; Fig. 2.5) with a slope of 1.57 ± 0.10 . Statistically significant correlations ($p \ll 0.001$) were also observed between DMS and DMSP ($r = 0.52$), and between DMSO and DMSP ($r = 0.60$), although the strength of these correlations was weaker than that observed between DMS and DMSO.

2.3.3 Turnover rate constants

Through our isotope tracer experiments, we were able to quantify turnover rate constants (d^{-1}) for DMS, DMSP and DMSO at a total of 20 stations. Table 2.1 summarizes the DMS/P/O concentrations and turnover rate constants obtained for each incubation station, while Fig. 2.6 shows the spatial distribution of the turnover rate constants. Across all 20 stations, rate constants for DMSO reduction averaged $0.079 \pm 0.015 d^{-1}$ (0.015 - 0.29 d^{-1}) and were comparable with those for DMSP cleavage ($0.084 \pm 0.012 d^{-1}$, ranging 0.019 - 0.10 d^{-1}). Relative to DMSO reduction and DMSP cleavage, turnover rate constants for net DMS change and gross DMS consumption were higher ($2.7 \pm 0.3 d^{-1}$ and $-1.4 \pm 0.3 d^{-1}$). A comparison of the measured concentrations, rate constants and various ancillary variables along the cruise track is presented in Fig. 2.7.

Since the seawater samples used to obtain initial DMS/P/O concentrations at each incubation station were not pre-filtered, concentrations reflect potential contributions from both the particulate and dissolved pools. In contrast, the turnover rate constants derived from our isotope tracer experiments capture a dominant signal from the dissolved pool. For this reason, turnover rates (computed as the product of rate constants and concentrations) were subject to significant uncertainty and thus not calculated (see discussion).

2.3.4 Sea-air flux

Sea-air fluxes of DMS along our cruise track averaged at $5.2 \pm 0.7 \mu\text{mol m}^{-2} \text{d}^{-1}$, in good agreement with previous studies in the same study area (Asher et al. 2011b; Herr et al. 2019). Daily wind speeds obtained from the CCMP wind vector analysis products were relatively low and homogeneous over our sampling area in the late summer (averaged wind speeds: $3.6 \pm 0.2 \text{ m/s}$). Hence, DMS fluxes were tightly correlated with DMS concentrations. Maximum sea-air fluxes were observed near the La Perouse Bank and QCS, consistent with the locations of DMS hotspots.

2.3.5 Comparison of distinct hydrographic domains

Results from PCA and k-mean clustering analysis revealed that our sampling stations clustered into two dominant groups that were separated across the 200 m isobath (Fig. 2.8). Stations along the deeper slope waters within the WCVI and QCS regions clustered together hydrographically, while the continental shelf WCVI stations and estuarine waters of the SoG formed a distinct group. In this analysis, we found that the first two PCA axes explained 67% of the total variability. Average values of different oceanographic properties across the two groups (defined as slope waters and shelf waters) are compared in Fig. 2.9. The slope stations were nitrate

depleted ($\text{NO}_3 = 0.02 \pm 0.02 \mu\text{M}$), whereas the shelf stations had higher NO_3 concentrations ($5.7 \pm 2.3 \mu\text{M}$). Nitrate concentrations within the two groups were determined to be statistically different ($p \ll 0.001$). Silicate concentrations in the two domains were similar, with greater variability in the slope (slope: $22 \pm 20 \mu\text{M}$; shelf: $21 \pm 5 \mu\text{M}$; $p = 0.9948$, Permutation test). The two groups were also characterized by different phytoplankton community structures. The slope stations were nano- and pico- phytoplankton dominated (relative abundance of sum of nano- and pico-phytoplankton in slope and shelf waters of $60 \pm 2\%$ and $27 \pm 3\%$), whereas continental shelf waters had a significantly higher fraction of diatoms (offshore: $10 \pm 3\%$; inshore: $38 \pm 5\%$). The difference in phytoplankton taxonomic abundances was statistically significant between the two groups of stations (nano- and pico-phytoplankton %: $p \ll 0.001$; diatom %: $p \ll 0.001$).

As with surface water hydrography, *in-situ* sulfur concentrations demonstrated distinct patterns between the two oceanographic domains. Higher values of chlorophyll-normalized DMSP_t and DMSO_t concentrations were observed in the slope waters ($\text{DMSP}_t/\text{Chl } a = 172 \pm 23 \text{ nmol } \mu\text{g}^{-1}$, $\text{DMSO}_t/\text{Chl } a = 10 \pm 2 \text{ nmol } \mu\text{g}^{-1}$) relative to the continental shelf waters ($\text{DMSP}_t/\text{Chl } a = 56 \pm 12 \text{ nmol } \mu\text{g}^{-1}$, $\text{DMSO}_t/\text{Chl } a = 2.7 \pm 0.9 \text{ nmol } \mu\text{g}^{-1}$). These regional differences between $\text{DMSP}_t/\text{Chl } a$ and $\text{DMSO}_t/\text{Chl } a$ were statistically different ($\text{DMSP}_t/\text{Chl } a$: $p \ll 0.001$; $\text{DMSO}_t/\text{Chl } a$: $p \ll 0.001$). Despite differences in nutrient supply and phytoplankton community structure in the two domains, turnover rate constants for net DMS production from DMSP cleavage ($k_{\text{DMSPcleav}}$) and DMSO reduction (k_{DMSOred}) were statistically similar. $k_{\text{DMSPcleav}}$ in slope and shelf waters averaged $0.10 \pm 0.02 \text{ d}^{-1}$ and $0.070 \pm 0.013 \text{ d}^{-1}$ ($p = 0.2991$), while k_{DMSOred} in two domains averaged $0.056 \pm 0.013 \text{ d}^{-1}$ and $0.097 \pm 0.024 \text{ d}^{-1}$ ($p = 0.1388$), respectively.

2.4 Discussion

Our study contributes new data on the concentrations and turnover rate constants of DMS, DMSP and DMSO in the waters adjacent to Vancouver Island, BC. This region is notable in terms of its high primary productivity and elevated concentrations of various reduced sulfur compounds, and for its high spatial heterogeneity, which results from complex physical dynamics and the influence of localized freshwater inputs. Here, we discuss the potential biotic and abiotic drivers of DMS/P/O concentrations and turnover rate constants across the two distinct hydrographic regions in our study area.

2.4.1 DMS/P/O concentrations around Vancouver Island

The range of surface DMS concentrations measured during our September, 2019 cruise (<0.1 to 31 nM, average of 6.2 nM) are more than twice the global median DMS concentration (2.4 nM), reflecting a regional DMS hotspot in the Northeast Pacific. Indeed, similarly elevated DMS concentrations have previously been reported from the same study area (e.g., Nemcek et al. 2008: average 5.8 nM; Tortell et al. 2012: 5.2 nM in 2007 and 10.2 nM in 2010; Asher et al. 2017b: 9.7 nM in coastal waters; Herr et al. 2019: 4.6 nM in the California Upwelling Coastal Province). Measurements of DMSP and DMSO in our study area are less common, and there are correspondingly fewer data for comparative purposes. Using the underway OSSCAR system, we measured DMSP_t concentrations ranging from ~1 nM to > 500 nM. By comparison, Herr et al. (2019) observed DMSP concentrations ranging from 26-480 nM, with the highest values found near the La Perouse Bank, which is consistent with our observations. To our knowledge, only four studies have previously reported *in-situ* DMSO concentrations in this study area (Bates et al. 1994; Asher et al. 2015, 2017b; Herr et al. 2020). Values from these previous studies range from 0-20

nM, in good agreement with our results. Moreover, the strong correlation between DMS and DMSO (Fig. 2.5) with a slope close to 1 is also consistent with previous observations (Hatton et al. 2004; Herr et al. 2020). Thus, a reasonably clear picture is now emerging of our study region as a persistent hotspot of DMS/P/O concentrations. It remains less clear, however, which factors are responsible for these elevated concentrations.

The spatial distribution of underway DMS/P/O measurements (Fig. 2.4) reveals higher values for all three sulfur compounds in continental shelf waters, specifically in regions influenced by riverine input (e.g., QCS: Rivers Inlet; WCVI: Nootka Sound and Barkley Sound; Fig. 2.1) and those characterized by SSHA (Fig. 2.8b). Lower SSHA values in near-shore waters is indicative of coastal upwelling, which brings nutrient-rich deep waters up to the surface and stimulates mixed layer primary productivity. The observation of elevated DMS concentrations in proximity to regions of low SSHA and riverine inputs, suggests the influence of macro- and micro-nutrients from coastal upwelling and/or riverine inputs in driving the variability of DMS distribution. At the same time, Herr et al. (2019) have previously observed high DMS concentrations associated with positive SSHA, caused by the warm-core Haida and Sitka eddies in the transitional waters. Such eddies have been shown to provide an additional mechanism to deliver nutrients offshore (Crawford 2002; Keith Johnson et al. 2005). As a result, both positive (indicative of warm-core eddies) and negative (indicative of coastal upwelling) SSHA may be associated with increased productivity and enhanced DMS concentrations. In a recent analysis of all available DMS data from the NE Pacific based on machine learning methods, McNabb et al., (in prep) found a strong regional imprint of SSHA features on DMS distributions.

In contrast to the WCVI and QCS regions, DMS/P/O concentrations in the SoG were generally low (Fig. 2.4a & 2.7a; e.g., DMS in the SoG = 2.8 ± 0.2 nM vs. 6.2 ± 0.5 nM for the

entire study area). To our knowledge, only one study has previously measured DMS/P concentrations in these estuarine waters (Sharma et al. 2003). During the late summer (August) period, these authors found DMS/P concentrations ranging from 0.5-14.2 nM and 10.2-284.7 nM, respectively, in good agreement with our observations (DMS = 0.34-4.4 nM, DMSP_t = 8.2-112 nM). These earlier results, taken at a later phase of the annual productivity cycle, suggest that relatively low DMS/P concentrations may be a persistent feature of the SoG. The lower sulfur concentrations in this region relative to the WCVI and QCS may result from a lower proportion of high DMSP- and DMSO-producing phytoplankton groups. Indeed, pigment analysis in the SoG shows that the relative percentage of dinoflagellates in the SoG stations was only 1.5 ± 0.3 % of total Chl *a*, with prasinophytes and diatoms dominating phytoplankton assemblages in these waters ($30 \pm 2\%$ and $28 \pm 2\%$, respectively; Fig. 2.7c). These latter phytoplankton groups produce much lower cellular DMSP than dinoflagellates (Stefels et al. 2007).

2.4.2 DMS - DMSO Relationship

Our results indicate a strong positive linear relationship between DMS and DMSO at concentrations below 20 nM (Fig. 2.5), confirming previous observations (Hatton et al. 2004; Herr et al. 2020). Notably, Herr et al. (2020) reported a DMSO to DMS ratio (DMSO:DMS = 0.92, during May, 2017) that was approximately two-fold higher than what we observed during late summer (DMSO:DMS = 0.42, Fig. 2.5). This difference may be attributable to several factors. First, lower light levels and reduced sunlight hours during our sampling period relative to that of Herr et al. (2020) could have decreased the intrinsic photochemical oxidation of DMS to DMSO (Hatton et al. 2004; del Valle et al. 2009). As shown in Fig. C.3.1, the average monthly PAR in September, 2019 ($27 \text{ E m}^{-2} \text{ day}^{-1}$) was $\sim 30\%$ lower than in May, 2017 ($40 \text{ E m}^{-2} \text{ day}^{-1}$). In addition,

lower primary productivity during our late summer cruise relative to the spring cruise of Herr et al. (2020) may also have indirectly decreased DMS photo-oxidation by reducing the supply of chromophoric dissolved organic matter (CDOM), which has been implicated in driving this process (Bouillon and Miller 2004; Bouillon et al. 2006; Taalba et al. 2013). Indeed, the average monthly CDOM absorbance in September, 2019 was nearly half of that in May, 2017 (0.044 m^{-1} vs. 0.074 m^{-1}) (Nelson and Siegel 2013; Appendix C, Fig. C.3.2). Taken together, differences between spring and late summer in light intensity and phytoplankton-derived CDOM concentrations could explain the relatively lower DMSO concentrations (and thus lower DMSO:DMS ratio) we measured relative to that reported by Herr et al. (2020).

Beyond potential differences in photo-oxidation (light and CDOM), lower bacterial oxidation of DMS to DMSO may also have contributed to the lower DMSO accumulation we observed. In support of this hypothesis, measured rate constants of DMS oxidation were below our detection limit at 2 out of 3 incubation stations (Appendix C, Fig. C.3.3), whereas Herr et al. (2020) reported a strong coupling between DMSO reduction and DMS oxidation, suggesting a stronger biological DMSO production term in their study. We thus conclude that lower DMSO production (both biotic and abiotic) can likely explain the lower DMSO concentrations we observed during late summer.

2.4.3 Sulfur cycling in slope and shelf waters

Our survey covered hydrographically distinct regimes, from continental slope waters with bottom depths greater than 2000 m, to shelf and estuarine waters with bottom depths of ~ 200 m or less. Sulfur cycling in these distinct regimes is likely influenced by a variety of environmental

factors, as demonstrated by our PCA analysis and k-mean clustering, which shows a clear hydrographic separation of our incubation stations across the continental shelf (Fig. 2.8).

Slope stations were dominated by high DMSP- and DMSO-producing dinoflagellates and prymnesiophytes (Fig. 2.9c), whereas the shelf stations were dominated by low DMSP/ DMSO-producing diatoms (Fig. 2.9d). As a result, $\text{DMSP}_t/\text{Chl } a$ and $\text{DMSO}_t/\text{Chl } a$ were significantly higher at the offshore, nano- and pico-phytoplankton dominated stations (Fig. 2.9e and f). However, rate measurements reveal statistically similar values of $k_{\text{DMSPcleav}}$ (Fig. 2.9g, $p = 0.2991$) and k_{DMSOred} (Fig. 2.9h, $p = 0.1388$) between the two clusters.

Previous work by Royer et al. (2010) has demonstrated lower DMSP-S assimilation efficiencies at offshore stations relative to inshore waters along the Line P transect (from the WCVI to Ocean Station Papa in the NE Subarctic Pacific). Offshore waters in our study region are typically nutrient depleted (mean NO_3 concentration of $0.02 \mu\text{M}$ at offshore stations vs. $5.72 \mu\text{M}$ at nearshore stations) and the bacterial productivity is likely limited by the availability of organic carbon (Hale et al. 2006; Royer et al. 2010), resulting in a lower bacterial sulfur demand. Under these conditions, the microbial community may decrease the relative proportion of DMSP used as a carbon source through the demethiolation/demethylation pathway, and thus leading to a greater fraction of DMSP being consumed via the cleavage pathway, liberating DMS as a less readily used sulfur source (Kiene et al. 2000; Simó 2001). At the shelf stations where nutrient stress is relaxed by coastal upwelling and river inputs, the availability of organic carbon is enhanced, thus promoting the assimilation of sulfur into bacterial proteins through the MeSH-producing pathway (Kiene and Linn 2000; Kiene et al. 2000; Simó 2001; Lizotte et al. 2009; Royer et al. 2010). This higher assimilation of reduced sulfur into proteins would, in turn, lead to the lower rate constants of bacterial DMSP cleavage in the shelf waters (Fig. 2.9g). On average, we did see a higher average

DMSP cleavage rate constant in the further offshore waters over the continental slope, though this difference was not statistically significant. In future studies, greater sampling coverage across the inshore – offshore nutrient gradient may be required for higher statistical confidence.

Relative to DMSP cleavage, it is more difficult to interpret the turnover rate constants of DMSO reduction, as there are more uncertainties in these experiments, and more limited understanding of the DMSO reduction pathway. As DMSO exhibits high cellular permeability (Tanaka et al. 2001; Spiese et al. 2009), isotopically labelled DMSO can be accessed by both phytoplankton and bacteria, such that k_{DMSOred} reflects the contribution of both autotrophic and heterotrophic microbes. Although several studies have measured species-specific cellular DMSO synthesis in phytoplankton (Simó et al. 2000; Hatton and Wilson 2007; Spiese et al. 2009), few studies have investigated DMSO reduction by different phytoplankton groups. Nonetheless, this activity seems to be broadly distributed across marine phytoplankton, albeit with significant differences across even closely related species (Spiese et al. 2009). By comparison with phytoplankton, far less information is available on bacterial DMSO reduction and its potential drivers (Hatton et al. 2004). Several studies have identified bacterial DMS oxidation to DMSO as an important transformation pathway for DMS in surface seawaters (Hatton et al. 2012; Lidbury et al. 2016), but, to our knowledge, no study has exclusively investigated bacterial DMSO reduction in oxygenated seawaters. Given the limited understanding of bacterial DMSO metabolism in the marine sulfur cycle, it remains challenging to interpret the patterns observed in k_{DMSOred} between the shelf and slope waters of the study region. As with DMSP cleavage, additional measurements across coastal-offshore gradients may provide greater statistical support for the apparent trend towards higher DMSO reduction in coastal waters (Fig. 2.9h).

2.4.4 Comparison with previous rate measurements and methodological considerations

2.4.4.1 Comparison with rate measurements in the same area

A key objective of this study was to directly compare the potential contributions of DMSP and DMSO as sources of DMS. On average, we found that the turnover rate constants for net DMS production from DMSO reduction were similar with those from dissolved DMSP cleavage in both hydrographic regimes (Fig. 2.9g and h; overall mean $k_{\text{DMSOred}} = 0.079 \pm 0.015 \text{d}^{-1}$, overall mean $k_{\text{DMSPcleav}} = 0.084 \pm 0.012 \text{d}^{-1}$, $p = 0.5861$). After taking into account differences in calculation procedures, this observation is similar to that of Herr et al. (2020). As noted in the methods, the calculation used by Herr et al. (2019, 2020) and Asher et al. (2017a; b) results in values that are ~100-fold higher than the approach taken here, which factors in the starting concentration of the tracer. After correcting results from Herr et al. (2020), we derive a mean k_{DMSOred} of $0.16 \pm 0.02 \text{d}^{-1}$ and $k_{\text{DMSPcleav}}$ of $0.19 \pm 0.03 \text{d}^{-1}$ during the May/June La Perouse cruise. These values are on the same order, though somewhat higher, than the rates we measured. The lower turnover rate constants for DMSP cleavage and DMSO reduction we measured could be due to seasonality of bacterial processes in the study area. Bacterial biomass in the coastal NE Pacific is typically higher in spring than in summer (Sherry et al. 1999), which may contribute to the faster rate constants for dissolved DMSP cleavage and DMSO reduction observed in Herr et al. (2020), as the reported rate constants are not normalized to bacterial biomass. As our rate measurements ($k_{\text{DMSPcleav}}$ and k_{DMSOred}) may potentially represent biological conversions by algal processes (discussed in *Section 2.4.4.3*), the higher net primary production in May/June, 2017 may also have contributed to the greater rate constants (CbPM model, $559 \text{ mg C m}^{-2} \text{d}^{-1}$ in May/June, 2017 vs. $260 \text{ mg C m}^{-2} \text{d}^{-1}$ in September, 2019).

2.4.4.2 Comparison with other tracer studies

Our work and that of other recent studies employing the same tracer-based method has revealed comparable biological DMS production from both dissolved DMSP cleavage and DMSO reduction pathways in different water masses with varying phytoplankton community structure (e.g., Asher et al. 2011, 2017b; Herr et al. 2020). In contrast, a recent study by Dixon et al. (2020) reported undetectable k_{DMSOred} over much of a seasonal cycle in May to October in temperate coastal waters of the N. Atlantic (salinity ~ 35 psu). Results from radiotracer incubations reported by these authors suggested that the majority of DMSO_d ($> 94\%$) was respired by the heterotrophic community for growth (Tyssebotn et al. 2017; Dixon et al. 2020), resulting in low or undetectable rates of DMSO reduction to DMS. In our study, DMSO reduction may have been triggered by nutrient stress, as part of a redox-coupled antioxidant cycle that includes DMSP, DMS and DMSO (Hatton 2002; Spiese et al. 2009). Going forward, given the sparse but highly variable measurements of DMSO reduction, additional studies simultaneously comparing different fates of DMSO (DMSO reduction to DMS, DMSO metabolism, DMSO oxidation to DMSO_2) are required to better constrain spatial and temporal variability in DMSO cycling.

2.4.4.3 Methodological considerations

The similar rate constants of k_{DMSOred} and $k_{\text{DMSPcleav}}$ (e.g., in the present study, and those of Asher et al. 2011a; Herr et al. 2020) may be partially due to the nature of uptake of different sulfur isotope tracers by phytoplankton and bacteria. DMSP is a zwitterion, which has a positively charged dimethyl group and a negatively charged carboxylate group. Membrane transport of such charged species requires binding proteins (Yoch et al. 1997). Vila-Costa et al. (2006) investigated uptake of radio-labelled DMSP by axenic phytoplankton cultures and natural communities,

showing that this compound can be assimilated by phytoplankton. These authors also noted that the relative proportion of DMSP assimilation by heterotrophic bacteria and phytoplankton depends on light conditions (e.g., greater proportional DMSP uptake by phytoplankton in the light). This result suggests that our tracer-based measurements would have reflected contributions of DMSP uptake and cleavage by both phytoplankton and bacteria, though the relative contributions of these two groups is difficult to determine. In contrast to DMSP, uncharged DMSO molecules have a high cellular membrane permeability (Tanaka et al. 2001; Spiess et al. 2009), such that the dissolved tracer of DMSO added to the incubation samples was likely accessible by both phytoplankton and bacteria. Our measured k_{DMSOred} is thus likely to represent something closer to community-wide DMSO reduction.

It is important to note that we only measured the turnover rate constants (unit: d^{-1}) of sulfur transformations in the dissolved pool. To compare the relative contribution of net DMS production from DMSP_d cleavage and DMSO_d reduction, dissolved DMSP and DMSO concentrations are needed for the calculation of turnover rates (unit: nM d^{-1}). In our study, we collected unfiltered DMS/P/O samples at each incubation station, and used total DMSO concentrations to calculate turnover rates of DMSO reduction in the dissolved pool. Given the high cellular membrane permeability of DMSO (Tanaka et al. 2001), we assume the total DMSO was accessible to microbes (Herr et al. 2020). To estimate turnover rates of DMSP cleavage, we adopted the reported ratio of DMSP_d and DMSP_t (3.64% DMSP_d of total DMSP) at inshore stations in our study area by Royer et al. (2010), and estimated the DMSP_d concentrations for microbial DMSP cleavage rates (Table 2.2). This approach provides only a rough approximation, given the potentially significant variability in the relative $\text{DMSP}_d : \text{DMSP}_t$ ratio (Royer et al. 2010; Asher et al. 2017b). Noting these caveats, we nonetheless estimated average rates of net DMS production from

bacterial DMSP cleavage and DMSO reduction as $0.30 \pm 0.10 \text{ nM d}^{-1}$ and $0.28 \pm 0.06 \text{ nM d}^{-1}$. These similar rates of DMSP cleavage and DMSO reduction further suggests that biological DMSO reduction may be an important source of net DMS production, particularly in coastal and estuarine waters where DMSO reduction turnover may be relatively faster (Fig. 2.9h).

2.4.4.4 DMS budget and mass balance

Based on our measurements, we constructed an approximate mass balance for net DMS production (Table 2.2). Net DMS production rate is directly measured in our experiments, as the change of unlabelled DMS concentrations over time ($m/z = 63$). If we assume: i) tracer DMSP was only accessible to the dissolved pool, albeit the potential component of phytoplankton contribution discussed above; ii) tracer DMSO was accessible to both phytoplankton and bacteria due to its high membrane permeability, the contribution of net DMS production attributable to bacterial DMSP cleavage and DMSO reduction is expressed as:

$$k_{DMSPcleav} \times DMSP_d + k_{DMSOred} \times DMSO_t$$

Net DMS production by other biological processes is:

$$\Delta net \text{ DMS production} = k_{DMS} \times DMS - k_{DMSPcleav} \times DMSP_d + k_{DMSOred} \times DMSO_t \quad \text{Eq.3}$$

where k_{DMS} is rate constant for net DMS production.

In our experiments, we found that the proportional contribution of total bacterial DMSP cleavage and DMSO reduction rates to net DMS production rates varied from 3.6% to 52% (mean $18 \pm 4 \%$). This large range likely represents true environmental variability, but may also partially reflect uncertainty in the DMSP cleavage term. In particular, it is not clear in our experiments what fraction of dissolved vs. particulate DMSP is reflected in our $k_{DMSPcleav}$ measurements. It seems likely, however, that the discrepancy between overall net DMS production, and that measured with

our tracers is likely due to algal production of DMS from intracellular DMSP cleavage and DMSO reduction, in addition to other biological DMS production pathways that were not measured in our study (e.g. photo-chemical conversions and zooplankton releases; Kiene and Linn 2000; Stefels et al. 2007).

2.4.4.5 Implication of DMSO reduction in contribution to DMS production

This study, and previous studies which used the same stable isotope tracers to simultaneously measure DMS production from DMSP cleavage and DMSO reduction (Asher et al. 2011a, 2017a; b; Herr et al. 2019, 2020), have suggested that biological DMSO reduction is an important contributor to DMS production. Whereas the rate constants (d^{-1}) for $k_{DMSP_{cleav}}$ and $k_{DMSO_{red}}$ were statistically similar in our dataset, the rates ($nM d^{-1}$) of DMS produced from DMSP cleavage and DMSO reduction are largely subject to concentrations of DMSP and DMSO. Total DMSP concentrations are typically higher than total DMSO concentrations in surface waters, due to higher $DMSP_p$ than $DMSO_p$ in algal cells, particularly in dinoflagellates and prymnesiophytes species (Hatton and Wilson 2007). Therefore, with the comparable rate constants for both pathways but significantly higher DMSP concentrations, net DMS gain from DMSP could be much more substantial than that from DMSO. However, in areas where DMSO is comparable to or higher than DMSP (e.g., oligotrophic tropical ocean by Zindler et al. 2013), biological DMSO reduction could be a dominant production pathway. In addition, since DMSO reduction is suggested to be a universal activity in marine phytoplankton, while DMSP lyase is only present in some species, DMSO reduction could be a major source of DMS production in those species lacking DMSP lyase activity (Spiese et al. 2009). Therefore, given the variability of global DMSP and DMSO distributions and algal functions (i.e., algal DMSP cleavage and DMSO reduction

activities), and the hypothesized antioxidant function of DMSO which may elevate DMS production under oxidative stress, it is important to evaluate the relative contributions of DMSP and DMSO to net DMS production in different hydrographic domains.

2.4.4.6 Future studies

In this study, we used a relatively new stable isotope tracer method to quantify DMS production from DMSO reduction and DMSP cleavage. These measurements provide only a partial understanding of the complex dynamics governing DMS cycling in seawater. In future studies, application of the tracer technique may be expanded to extend our understanding of this cycle. For example, additional measurements of the isotopically labelled methanethiol (MeSH) could be adopted to compare the relative proportion of DMSP consumption through demethylation/demethiolation vs. cleavage. In this approach, the appearance of deuterated D₃-MeSH derived from D₆-DMSP would represent the demethylation/demethiolation pathway, while the appearance of deuterated D₆-DMS from D₆-DMSP would represent the cleavage pathway. Since the generated D₆-DMS can be further degraded to D₃-MeSH, tracer ¹³C₂-DMS could be added to determine MeSH production from DMS degradation. In this experiment, the appearance of ¹³C-MeSH would represent MeSH production from DMS degradation, whereas the difference between D₃-MeSH and ¹³C-MeSH could be used to quantify the methanethiol production from the demethylation/demethiolation pathway. In this way, turnover of DMSP consumption through the demethylation/demethiolation pathway and cleavage pathways could be simultaneously evaluated.

Our study focused on *in-situ* biological transformations of DMS/P/O only, however, one can also take advantage of the stable isotope tracer method and study turnover of DMS photo-oxidation in the laboratory. For instance, turnover of DMS photo-oxidation can be examined by

conducting incubation experiments with stable isotope tracers in the dark vs. in the light. Furthermore, the effect of CDOM concentrations on DMS photolysis can also be determined by dark/light experiments.

2.5 Conclusion

This study reports DMS/P/O concentrations and turnover rate constants in the coastal subarctic NE Pacific, a global DMS production hotspot. Our results reveal a strong correlation between DMS and DMSO concentrations, and comparable turnover rate constants of DMSO reduction relative to DMSP cleavage, suggesting DMSO as an important contributor in marine DMS production. Our results also showed that distinct hydrographic regimes in slope and shelf waters differed significantly in sulfur concentrations, although less significantly in turnover rates among DMS/P/O. Greater sampling coverage of distinct hydrographic regimes is suggested to evaluate the difference in turnover of DMSP and DMSO in contribution of DMS production. Additional field sampling and laboratory-controlled studies are required to determine the physical and biological drivers of marine DMS production, and the response of various autotrophic and heterotrophic groups to oxidative stressors. In addition, as more recent studies have revealed important sulfur metabolites beyond DMS/P/O (e.g. Thume et al. 2018), extended understanding of various sulfur transformation pathways is needed for establishment of regional and global biogeochemical models.

Table 2.1 Summary of Chl *a* concentrations, total DMS/P/O concentrations and rate constants from 20 incubation stations. Error bars represent one standard error.

Station	Chlorophyll (ug/L)	DMS (nM)	DMSP _t (nM)	DMSO (nM)	k _{net} DMS change (d ⁻¹)	k _{gross} DMS consumption (d ⁻¹)	k _{DMSP} cleavage (10 ⁻² d ⁻¹)	k _{DMSO} reduction (10 ⁻² d ⁻¹)
LB01	3.1	12	117	5.7	-	-1.7 ± 0.1	-	10 ± 1
LB16	0.21	2.9	35	2.7	1.9 ± 0.5	-1.4 ± 0.1	-	4.5 ± 0.0
LC11	0.14	1.2	33	3.0	1.7 ± 0.7	-	5.6 ± 0.8	1.5 ± 0.4
LC01	2.3	3.9	119	4.7	3.8 ± 1.3	-1.8 ± 0.1	1.9 ± 0.3	-
LD01	13	13	423	18	1.8 ± 0.5	-1.4 ± 0.1	10 ± 1	-
LD11	0.24	1.0	38	2.8	-	-2.8 ± 1.0	3.9 ± 0.8	2.5 ± 0.1
LG09	0.33	0.59	40	2.5	4.0 ± 1.9	-	9.3 ± 0.3	4.4 ± 0.3
LJ06	0.32	0.94	66	1.9	5.5 ± 1.0	-1.4	17 ± 1	3.5 ± 0.1
LBP7	0.37	0.73	36	4.0	2.5 ± 0.8	-0.54	8.4 ± 0.5	9.0 ± 0.2
LBP3	0.50	2.7	48	5.2	2.0 ± 0.5	-	10 ± 1.0	2.0 ± 0.4
CPE2	-	1.4	81	3.8	2.8 ± 0.7	-	4.5 ± 0.3	11 ± 1.0
CS00	0.94	0.65	107	2.8	5.3 ± 1.4	-	18 ± 1	13 ± 1
CS04	1.4	2.1	150	3.8	2.1 ± 0.5	-1.9 ± 0.1	14 ± 2	7.7 ± 0.9
SS1	0.42	0.77	54	2.9	4.5 ± 0.4	-0.75	10 ± 1	6.5 ± 0.8
SS5	1.9	2.5	61	3.8	1.3 ± 2.8	-3.7 ± 0.5	8.6 ± 2.4	29 ± 2
CPE1	4.0	4.7	115	7.2	0.96	-1.2 ± 0.2	7.3 ± 0.8	4.1 ± 0.3
stn14	3.3	2.0	55	3.7	2.0 ± 0.2	-0.76	7.7 ± 1.0	11 ± 1
stn12	1.1	0.17	36	1.6	1.7 ± 0.3	-1.7	3.0 ± 0.3	7.0 ± 0.3
stn22	2.1	4.2	27	4.4	2.1 ± 0.7	1.7	2.3 ± 0.6	6.6 ± 1.1
CPF2	0.98	0.32	16	1.5	2.4	-1.9	-	9.1 ± 0.4

Table 2.2 Estimated DMS budget from biological production/consumption rates. Rates for DMSP_d cleavage are calculated by estimating DMSP_d : DMSP_t = 3.64% from Royer et al., (2010). Error bars represent one standard error.

Station	DMSP_dcleav (nM d⁻¹)	DMSOred (nM d⁻¹)	net DMS prod. (nM d⁻¹)	(DMSP_dcleav+DMSOred)/ net DMS prod. (%)	Δnet DMS prod. (nM d⁻¹)
LB01	-	0.60	-	-	-
LB16	-	0.12	5.6	-	-
LC11	0.067	0.046	2.1	5.4	2.0
LC01	0.082	-	15	-	-
LD01	1.58	-	23	-	-
LD11	0.054	0.069	-	-	-
LG09	0.13	0.11	2.4	10	2.1
LJ06	0.40	0.066	5.1	9.3	4.6
LBP7	0.11	0.36	1.7	27	1.3
LBP3	0.18	0.10	5.3	5.3	5.0
CPE2	0.13	0.41	3.9	14	3.3
CS00	0.71	0.36	3.4	31	2.4
CS04	0.76	0.29	4.4	24	3.3
SS1	0.21	0.19	3.5	11	3.1
SS5	0.19	1.1	3.3	40	2.0
CPE1	0.31	0.29	4.5	13	3.9
stn14	0.15	0.41	4.1	14	3.5
stn12	0.039	0.11	0.29	52	0.14
stn22	0.023	0.29	8.8	3.6	8.5
CPF2	-	0.14	0.75	-	-
Average	0.30 ± 0.10	0.28 ± 0.06	5.4 ± 1.3	18 ± 4	3.2 ± 0.5

* $DMSP_{d\text{cleav}}$ indicates rates of net DMS production from $DMSP_d$ cleavage. $DMSO_{red}$ indicates rates of net DMS production from DMSO reduction. Net DMS prod. indicates net DMS production rates. $(DMSP_{d\text{cleav}}+DMSO_{red})/\text{net DMS prod.}$ indicates percentage of our measured bacterial $DMSP$ cleavage and DMSO reduction in contribution to net DMS production rates. $\Delta\text{net DMS prod.}$ indicates the missing net DMS production rates in the DMS budget.

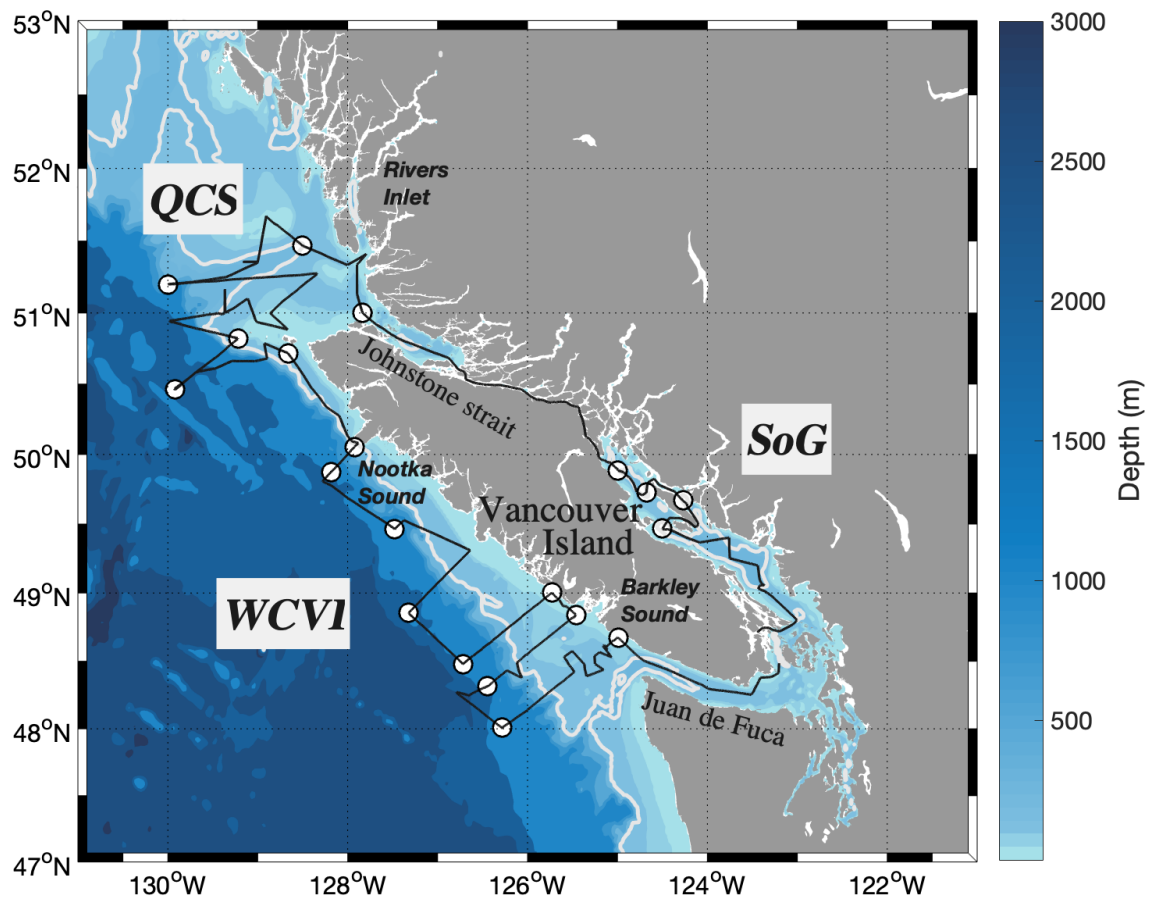


Figure 2.1 Ship track (black lines) and location of tracer experiments (white circles) from La Perouse cruise in September, 2019. WCVI, QCS and SoG denote West Coast of Vancouver Island, Queen Charlotte Sound and Strait of Georgia, respectively. Colormap represents bathymetry. The light grey solid line represents the 200m isobath.

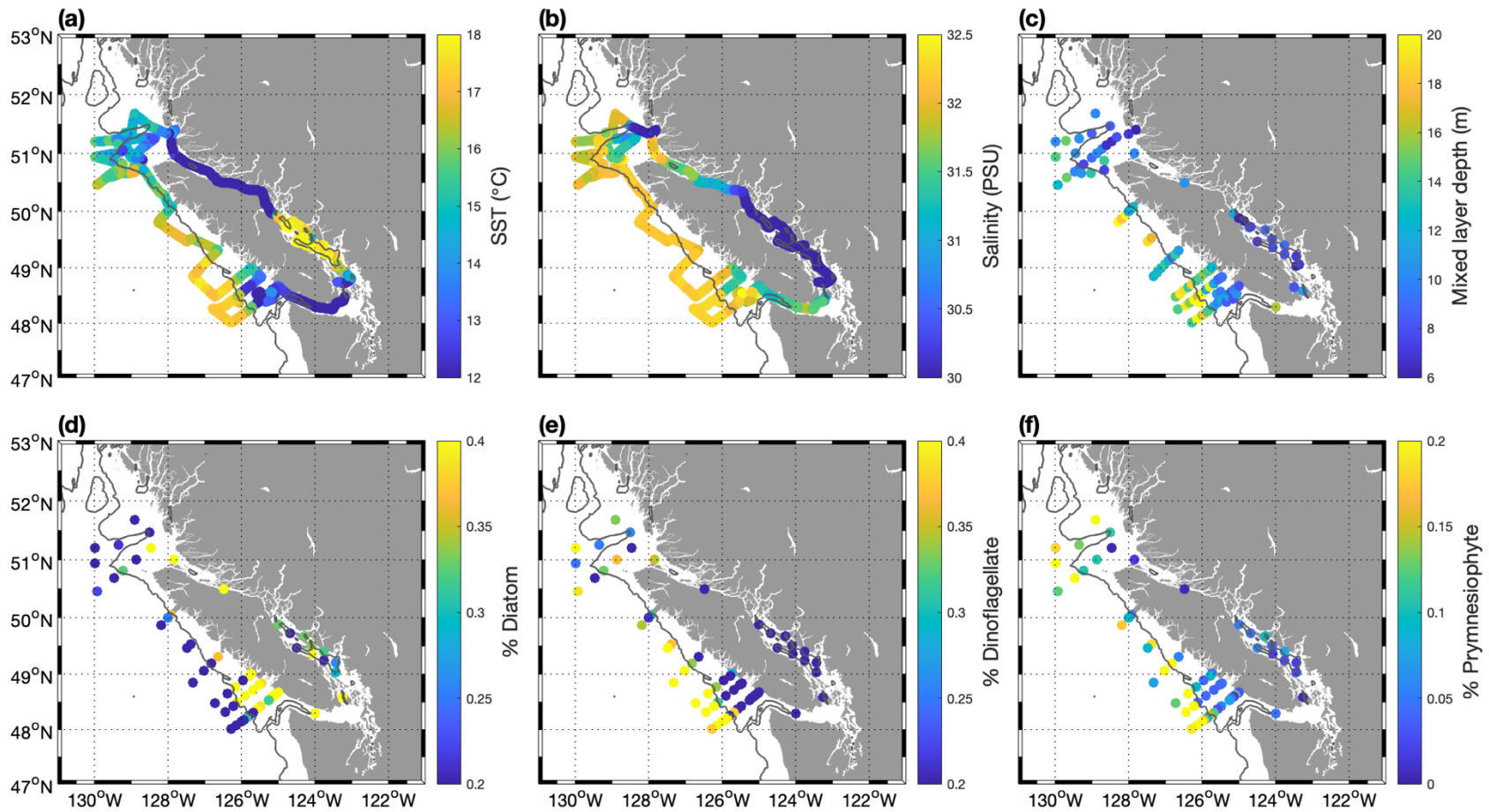


Figure 2.2 Distributions of (a) sea surface temperature (SST); (b) salinity; (c) mixed layer depths (MLD); and relative abundance of diatoms (d), dinoflagellates (e), and prymnesiophytes (f) derived from HPLC-based pigment analysis during the September, 2019 cruise. Grey solid lines represent the 200 m isobath.

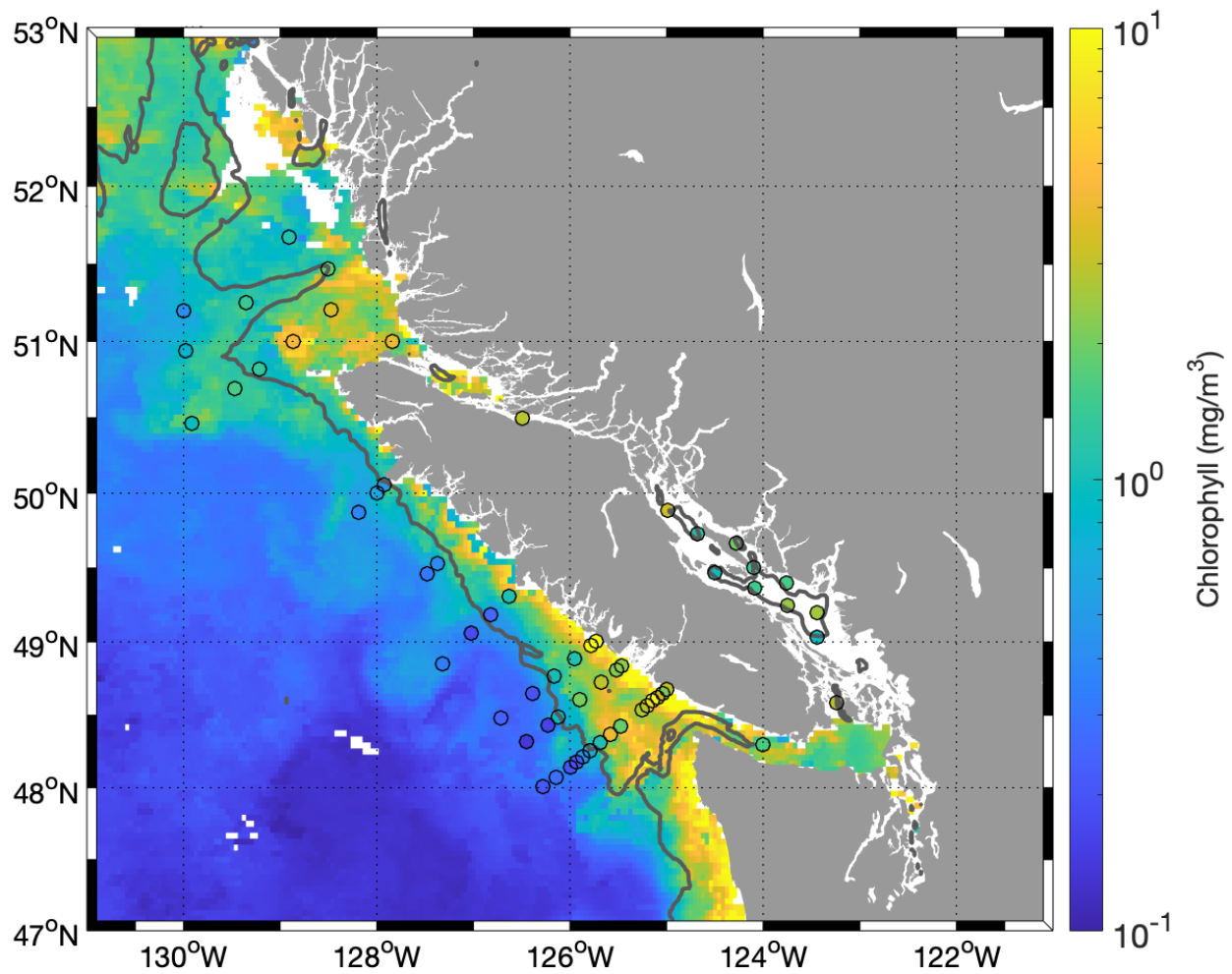


Figure 2.3 Comparison of discrete in-situ Chl *a* measurements (colored dots) and satellite-based Chl *a* measurements (background color) derived from the 8-day MODIS-Aqua satellite averaged from Aug 21-Sep 13, 2019. Colorbar scale is logarithmic. The grey solid line represents the 200 m isobath. The figure demonstrated good coherence between satellite and discrete Chl *a* data.

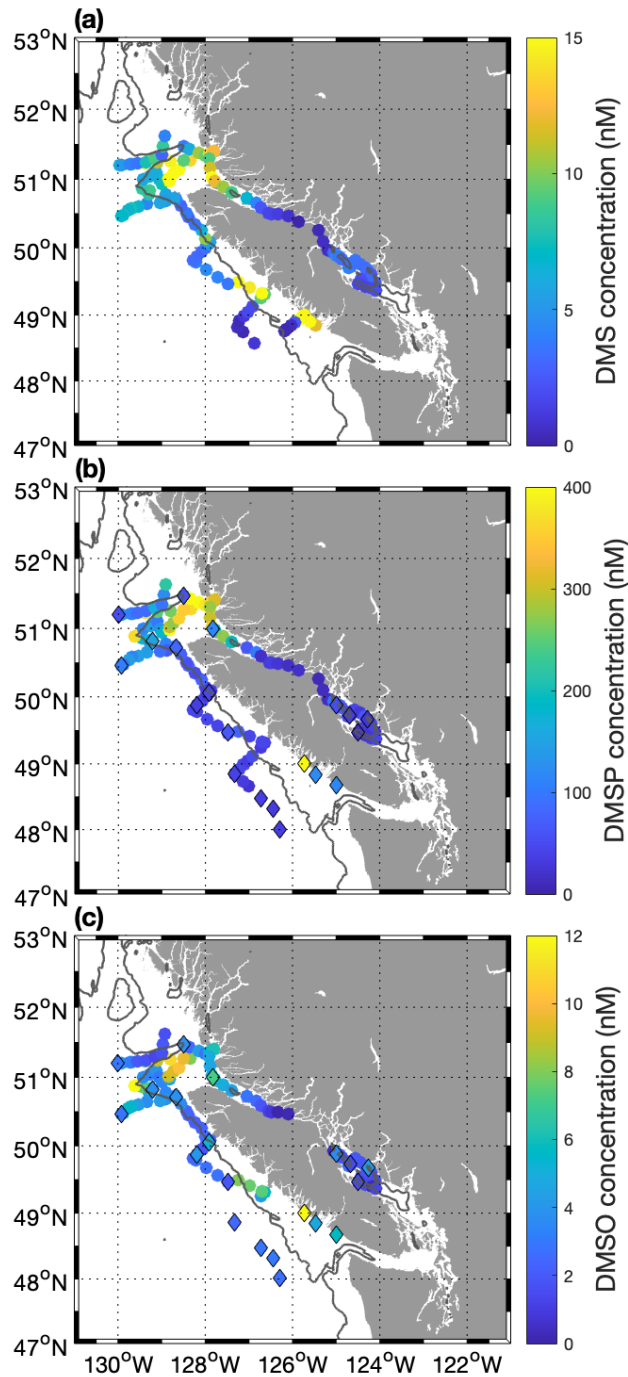


Figure 2.4 Concentrations of surface water (a) DMS, (b) DMSP and (c) DMSO around Vancouver Island in September, 2019. Round scatter points (●) are underway measurements from the automated OSSCAR system; diamond scatter points (◆) are discrete samples analyzed in the laboratory. Measurements for DMSP and DMSO are not available from the early cruise samples due to instrument problems.

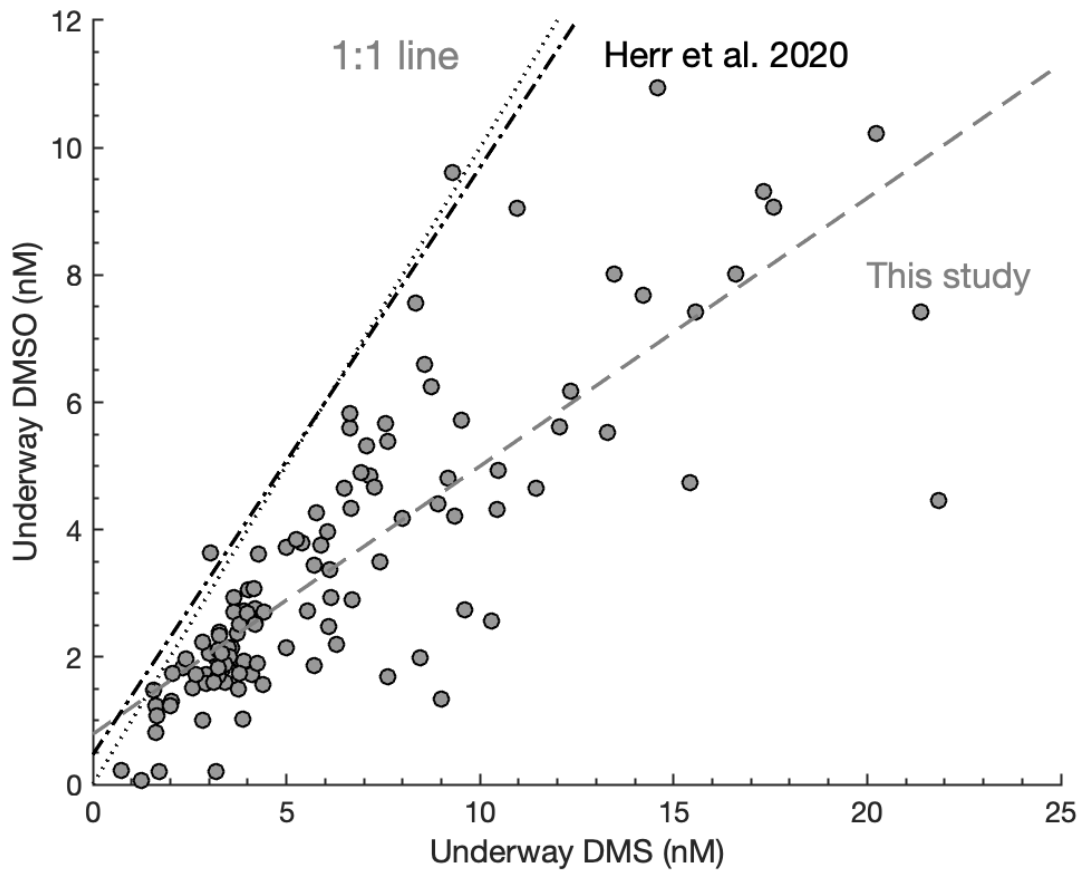


Figure 2.5 Linear relationship between DMS and DMSO concentrations around Vancouver Island during September, 2019. The black dashed line represents a linear fit to the data ($[DMSO_t] = 0.42 \times [DMS] + 0.79, r = 0.81, p \ll 0.001$). The dashed-dot line indicates the linear fit to the May, 2017 data obtained by Herr et al. (2020) ($[DMSO_t] = 0.92 \times [DMS] + 0.47, r = 0.77, p \ll 0.001$), and the black dotted line indicates a 1:1 relationship.

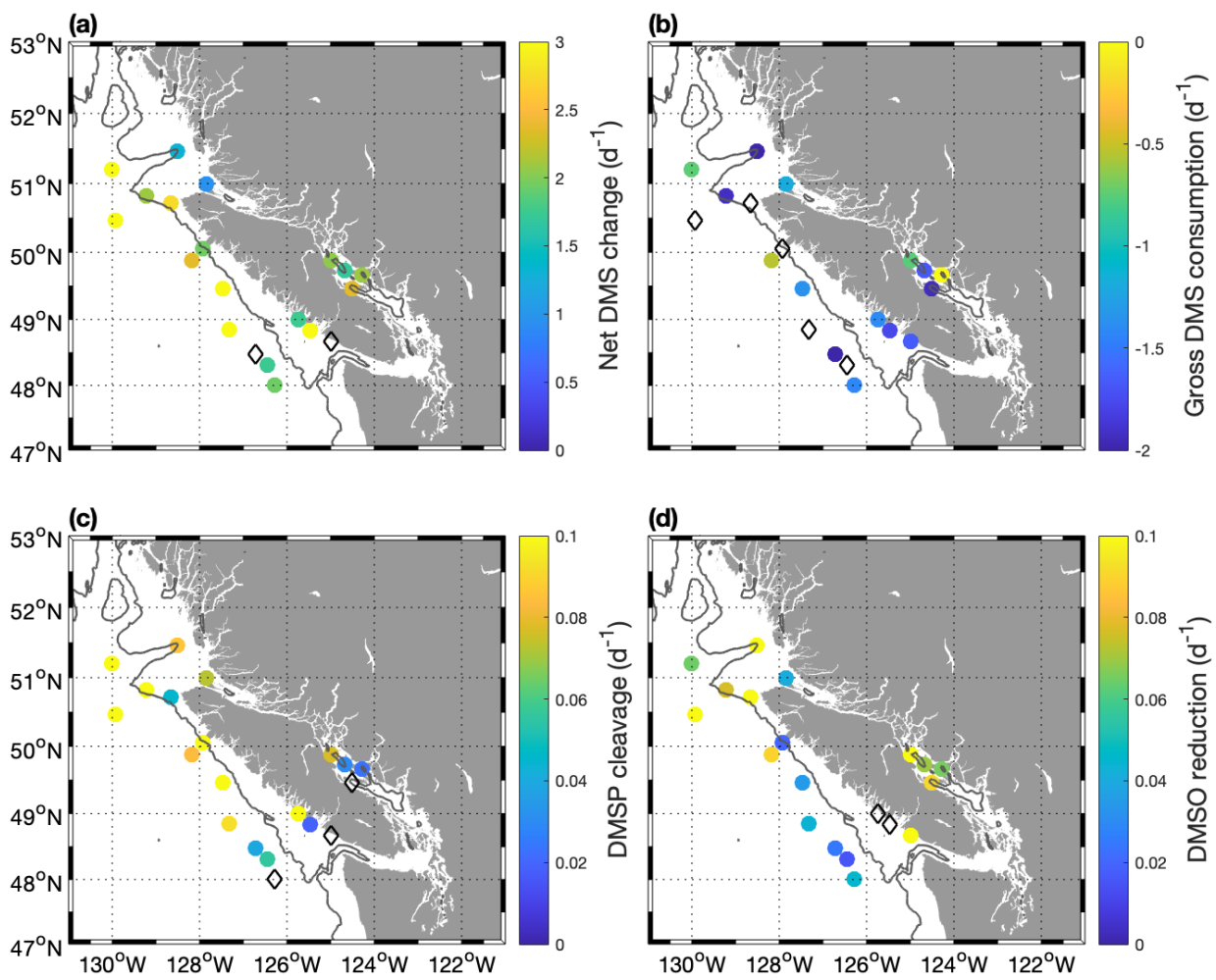


Figure 2.6 Rate measurements of (a) net DMS change, (b) gross DMS consumption, (c) DMS production from DMSP cleavage, and (d) DMS production from DMSO reduction. Rate constants below detection limit are shown as hollow symbols (\diamond). The grey solid line in each panel represents the 200 m isobath.

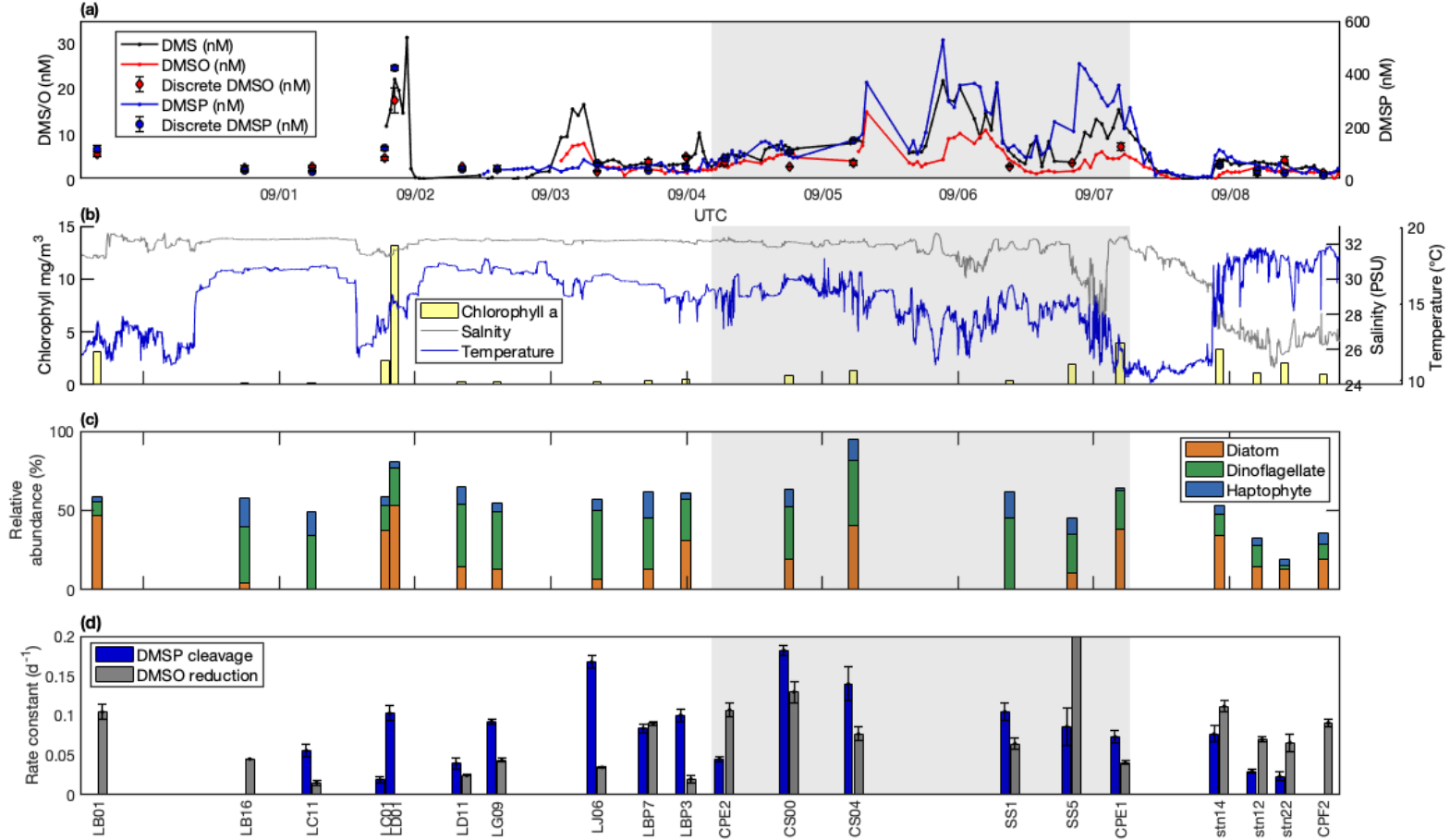


Figure 2.7 Ship-track distribution of (a) DMS/P/O concentrations; (b) sea surface salinity, temperature and discrete Chl *a* samples; (c) relative abundance of diatoms, dinoflagellates and haptophytes; and (d) turnover rate constants of DMSP cleavage and DMSO reduction. Note that the rate constant for DMSO reduction at station SS5 ($k = 0.29 \pm 0.02 \text{ d}^{-1}$) exceeds the y-scale, and is not plotted. Grey patches indicate the QCS region. Error bars represent one standard error.

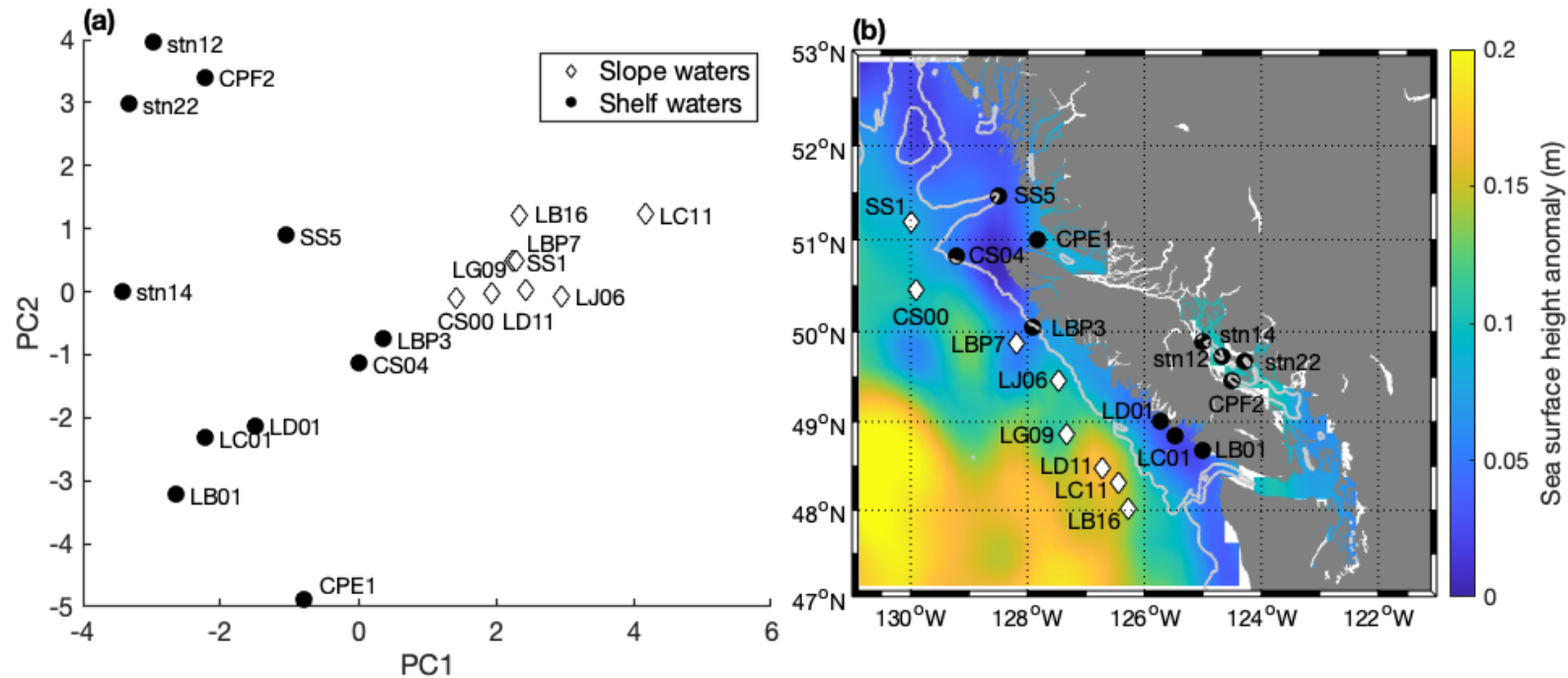


Figure 2.8 (a): Results from PCA and k-mean clustering analysis using Chl *a*, NO₃, PO₄, Si, salinity, temperature, density, MLD and relative abundance of different phytoplankton groups as input variables. The first two PC axes explain 67% of total variance of the dataset. Diamonds and circles represent two clustering ($k = 2$) groups; white diamond symbols in dark blue represent slope stations, and black round symbols in light blue represent on-shelf stations. (b): Locations of discrete incubation stations superimposed on the sea surface height anomaly derived from remote sensing observations. Grey solid line represents the 200 m isobath.

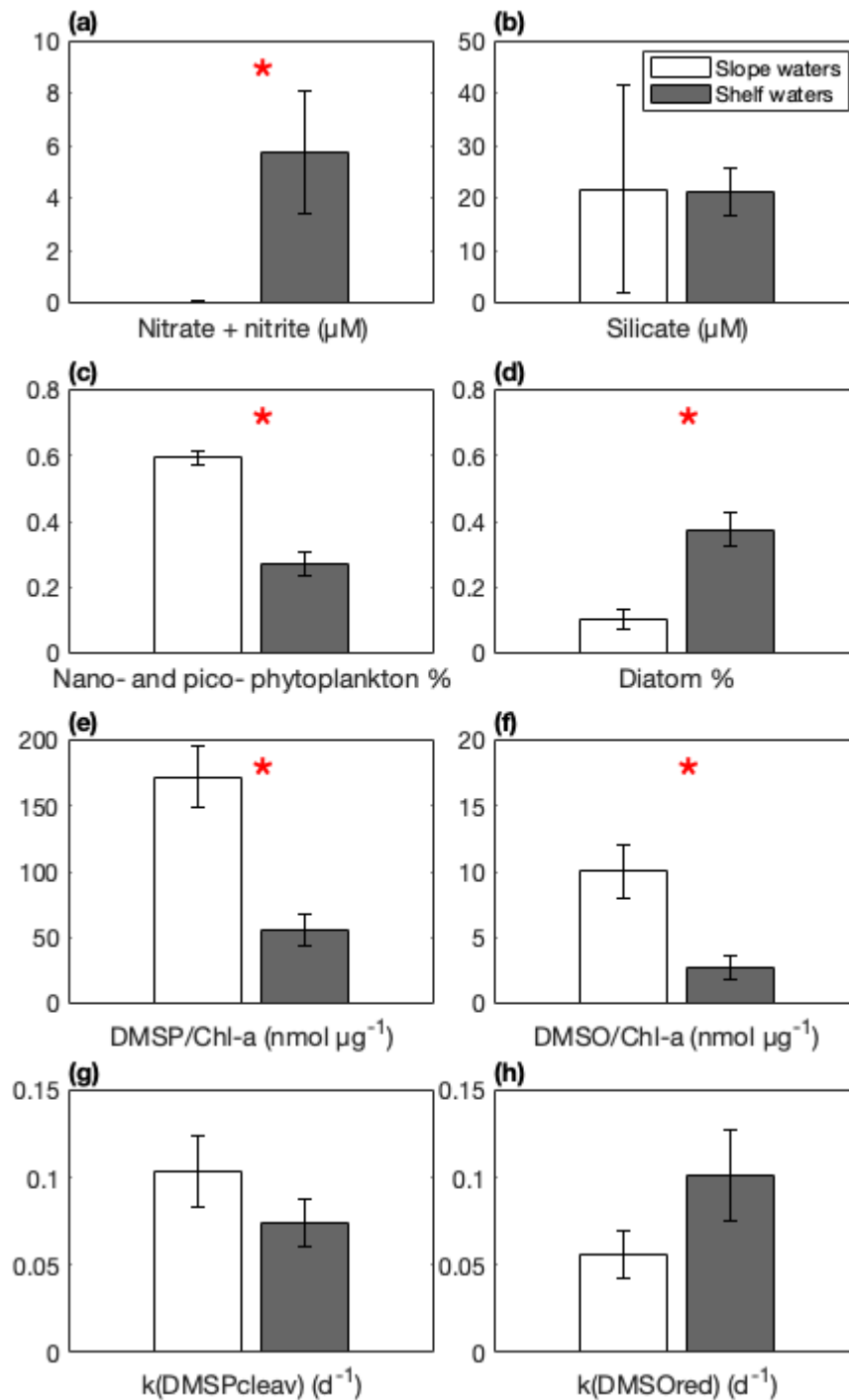


Figure 2.9 Comparison of various environmental variables, sulfur concentrations and rate constants between the slope and on-shelf stations. Variables with statistical differences between the two sets of stations are marked with a red asterisk. Error bars indicate one standard error.

Chapter 3: Conclusion

The main objective of this thesis was to further understand the factors driving variability in the concentrations and turnover rates of DMS, DMSP and DMSO in the coastal NESAP. In Chapter 2, I used an autonomous underway system developed by the Tortell group to measure distributions of surface DMS, DMSP and DMSO concentrations at high resolution. I also conducted rate measurements using a stable isotope tracer method to examine production and removal pathways of DMS. In the Appendices, I present supplementary materials from laboratory tests. Several DMSP preservation methods were investigated and optimized prior to our sampling mission in 2019 (Appendix A). Due to deficiency of DMSO reductase used for DMSO analysis, a TiCl_3 reduction method was also evaluated in the laboratory, and a detailed protocol is presented in Appendix B.

3.1 Major findings

In Chapter 2, high resolution DMS/P/O data further confirm the coastal subarctic NE Pacific as a global DMS hotspot. Concentration data show a tight coupling between DMS and DMSO, as previously observed, however, the DMSO:DMS ratio I observed was lower than earlier measurements. This result suggests that DMSO concentrations may be affected by several environmental factors, including light intensity, CDOM concentrations, and biological DMS oxidation. I also demonstrated comparable DMSO reduction rate constants in relative to DMSP cleavage rate constants in our study area, suggesting that DMSO may act as an important DMS precursor in addition to DMSP. Lastly, I applied statistical methods including PCA and k-mean clustering analysis to identify two hydrographic regimes (continental slope and shelf waters) in

my study area with distinct features of phytoplankton community structure, nutrient cycling and DMS/P/O concentrations but similar sulfur turnover rates. My results suggest that rate constants for net DMS production from DMSP cleavage and DMSO reduction were similar between the two hydrographically distinct regimes. Albeit the less statistically significant difference, the average $k_{\text{DMSPcleav}}$ was higher in shelf waters, which could be explained by the higher bacterial carbon and sulfur demand in the more productive shelf waters. On the other hand, it is challenging to interpret the patterns observed in k_{DMSOred} between the two domains, given the sparse studies on biological DMSO reduction.

3.2 Limitations and future outlook

Due to limited ancillary measurements, it is challenging for us to further interpret the results from turnover rate measurements and to draw broader biogeochemical conclusions. Future work should combine additional ancillary measurements to address remaining gaps in our understanding of the marine sulfur cycle. For instance, parallel measurements using a fast repetition rate fluorometer (FRRF) to measure the photosynthetic efficiency of photosystem II (Fv/Fm) and non-photochemical quenching (NPQ) could be adopted. The measurements of Fv/Fm and NPQ indicate oxidative stress experienced by phytoplankton cells, providing information about antioxidant function of cellular DMSO. On the DMSP side, further ancillary measurements on heterotrophic community are needed, such as bacterial productivity, bacterial abundance, and bacterial sulfur assimilation efficiency, as DMSP is an important food source for microbial community.

To my knowledge, only five studies have simultaneously compared biological DMSP cleavage and DMSO reduction *in-situ* (Asher et al. 2011a, 2017a; b; Dixon et al. 2020; Herr et al.

2020). Research attention has largely focused on marine DMS production by algal and bacterial DMSP cleavage and relevant driving factors. However, as more recent studies have revealed comparable DMS production pathway from DMSO reduction, it is suggested that biological DMSO reduction may serve as an important source of marine DMS. More intensive field sampling of DMSO distribution and cycling are needed, extending the spatial and temporal coverage of DMSO measurements in the global dataset. Laboratory-controlled experiments are also needed to evaluate the antioxidant function of DMSO, examining the response of DMSO reduction to various oxidative stressors (e.g., UV, Fe, Cu, macronutrients) in bacterial and phytoplankton cultures. It is also important to identify the difference of k_{DMSOred} between autotrophic and heterotrophic communities. Finally, understanding of marine sulfur cycle can also incorporate other organosulfur compounds, such as DMSOP, DMSO_2 , MeSH, extending our existing knowledge of marine sulfur cycle.

Bibliography

- Archer, S. D., K. Safi, A. Hall, D. G. Cummings, and M. Harvey. 2011. Grazing suppression of dimethylsulphoniopropionate (DMSP) accumulation in iron-fertilised, sub-Antarctic waters. *Deep Sea Res. Part II Top. Stud. Oceanogr.* **58**: 839–850. doi:10.1016/J.DSR2.2010.10.022
- Asher, E. C., J. W. H. Dacey, T. Jarníková, and P. D. Tortell. 2015. Measurement of DMS, DMSO, and DMSP in natural waters by automated sequential chemical analysis. *Limnol. Oceanogr. Methods* **13**: 451–462. doi:10.1002/lom3.10039
- Asher, E. C., J. W. H. Dacey, M. M. Mills, K. R. Arrigo, and P. D. Tortell. 2011a. High concentrations and turnover rates of DMS, DMSP and DMSO in Antarctic sea ice. *Geophys. Res. Lett.* **38**. doi:10.1029/2011GL049712
- Asher, E. C., J. W. H. Dacey, M. Stukel, M. C. Long, and P. D. Tortell. 2017a. Processes driving seasonal variability in DMS, DMSP, and DMSO concentrations and turnover in coastal Antarctic waters. *Limnol. Oceanogr.* **62**: 104–124. doi:10.1002/lno.10379
- Asher, E. C., A. Merzouk, and P. D. Tortell. 2011b. Fine-scale spatial and temporal variability of surface water dimethylsulfide (DMS) concentrations and sea–air fluxes in the NE Subarctic Pacific. *Mar. Chem.* **126**: 63–75. doi:10.1016/J.MARCHEM.2011.03.009
- Asher, E., J. W. Dacey, D. Ianson, A. Peña, and P. D. Tortell. 2017b. Concentrations and cycling of DMS, DMSP, and DMSO in coastal and offshore waters of the Subarctic Pacific during summer, 2010–2011. *J. Geophys. Res. Ocean.* **122**: 3269–3286. doi:10.1002/2016JC012465
- Barak-Gavish, N., M. J. Frada, P. A. Lee, and others. 2018. Bacterial virulence against an oceanic bloom-forming phytoplankter is mediated by algal DMSP. *Sci. Adv.* **4**: eaau5716. doi:10.1101/321398
- Barwell-Clarke, J., and F. Whitney. 1996. Institute of Ocean Sciences Nutrient Methods and

- Analysis, p. 43. *In* Canadian Technical Report of Hydrography and Ocean Sciences, No. 182.
- Bates, T. S., R. P. Kiene, G. V. Wolfe, P. A. Matrai, F. P. Chavez, K. R. Buck, B. W. Blomquist, and R. L. Cuhel. 1994. The cycling of sulfur in surface seawater of the northeast Pacific. *J. Geophys. Res.* **99**: 7835–7843. doi:10.1029/93JC02782
- Del Bel Belluz, J., M. A. Peña, J. M. Jackson, and N. Nemcek. 2021. Phytoplankton Composition and Environmental Drivers in the Northern Strait of Georgia (Salish Sea), British Columbia, Canada. *Estuaries and Coasts*. doi:10.1007/s12237-020-00858-2
- Bouillon, R.-C., and W. L. Miller. 2004. Determination of apparent quantum yield spectra of DMS photo- degradation in an in situ iron-induced Northeast Pacific Ocean bloom. *Geophys. Res. Lett.* **31**: L06310. doi:10.1029/2004GL019536
- Bouillon, R.-C., W. L. Miller, M. Levasseur, M. Scarratt, A. Merzouk, S. Michaud, and L. Ziolkowski. 2006. The effect of mesoscale iron enrichment on the marine photochemistry of dimethylsulfide in the NE subarctic Pacific. *Deep Sea Res. Part II Top. Stud. Oceanogr.* **53**: 2384–2397. doi:10.1016/j.dsr2.2006.05.024
- Boyd, P., and P. J. Harrison. 1999. Phytoplankton dynamics in the NE subarctic Pacific. *Deep Sea Res. Part II Top. Stud. Oceanogr.* **46**: 2405–2432.
- Bullock, H. A., H. Luo, and W. B. Whitman. 2017. Evolution of Dimethylsulfoniopropionate Metabolism in Marine Phytoplankton and Bacteria. *Front. Microbiol.* **8**: 637. doi:10.3389/fmicb.2017.00637
- Bylhouwer, B., D. Ianson, and K. Kohfeld. 2013. Changes in the onset and intensity of wind-driven upwelling and downwelling along the North American Pacific coast. *J. Geophys. Res. Ocean.* **118**: 2565–2580. doi:10.1002/jgrc.20194

- Challenger, F., and M. . Simpson. 1948. Studies on biological methylation; a precursor of the dimethyl sulphide evolved by *Polysiphonia fastigiata*; dimethyl-2-carboxyethylsulphonium hydroxide and its salts. *J. Chem. Soc.* **3**: 1591–1597.
- Charlson, R. J., J. E. Lovelock, M. O. Andreae, and S. G. Warren. 1987. Oceanic phytoplankton, atmospheric sulphur, cloud albedo and climate. *Nature* **326**: 655–661.
doi:10.1038/326655a0
- Crawford, W. R. 2002. Physical characteristics of Haida Eddies. *J. Oceanogr.* **58**: 703–713.
- Curran, M. A. J., G. B. Jones, and H. Burton. 1998. Spatial distribution of dimethylsulfide and dimethylsulfoniopropionate in the Australasian sector of the Southern Ocean. *J. Geophys. Res. Atmos.* **103**: 16677–16689. doi:10.1029/97JD03453
- Curson, A. R. J., J. Liu, A. Bermejo Martínez, and others. 2017. Dimethylsulfoniopropionate biosynthesis in marine bacteria and identification of the key gene in this process. *Nat. Microbiol.* **2**. doi:10.1038/nmicrobiol.2017.9
- Dacey, J. W. H., and N. V Blough. 1987. Hydroxide decomposition of dimethylsulfoniopropionate to form dimethylsulfide. *Geophys. Res. Lett.* **14**: 1246–1249.
doi:10.1029/GL014i012p01246
- Deschaseaux, E. S. M., R. P. Kiene, G. B. Jones, M. A. Deseo, H. B. Swan, L. Oswald, and B. D. Eyre. 2014. Dimethylsulphoxide (DMSO) in biological samples: A comparison of the TiCl_3 and NaBH_4 reduction methods using headspace analysis. *Mar. Chem.* **164**: 9–15.
doi:10.1016/J.MARCHEM.2014.05.004
- Dixon, J. L., F. E. Hopkins, J. A. Stephens, and H. Schäfer. 2020. Seasonal changes in microbial dissolved organic sulfur transformations in coastal waters. *Microorganisms* **8**: 1–20.
doi:10.3390/microorganisms8030337

- Freeland, H. J., W. R. Crawford, and R. E. Thomson. 1984. Currents along the Pacific coast of Canada. *Atmos. - Ocean* **22**: 151–172. doi:10.1080/07055900.1984.9649191
- Gunson, J. R., S. A. Spall, T. R. Anderson, A. Jones, I. J. Totterdell, and M. J. Woodage. 2006. Climate sensitivity to ocean dimethylsulphide emissions. *Geophys. Res. Lett.* **33**: 2–5. doi:10.1029/2005GL024982
- Hale, M. S., R. B. Rivkin, P. Matthews, N. S. R. Agawin, and W. K. W. Li. 2006. Microbial response to a mesoscale iron enrichment in the NE subarctic Pacific: Heterotrophic bacterial processes. *Deep. Res. Part II Top. Stud. Oceanogr.* **53**: 2231–2247. doi:10.1016/j.dsr2.2006.05.039
- Harris, S. L., D. E. Varela, F. W. Whitney, and P. J. Harrison. 2009. Nutrient and phytoplankton dynamics off the west coast of Vancouver Island during the 1997/98 ENSO event. *Deep. Res. Part II Top. Stud. Oceanogr.* **56**: 2487–2502. doi:10.1016/j.dsr2.2009.02.009
- Harrison, P. J., J. D. Fulton, F. J. R. Taylor, and T. R. Parsons. 1983. Review of the biological oceanography of the Strait of Georgia: pelagic environment. *Can. J. Fish. Aquat. Sci.* **40**: 1064–1094. doi:10.1139/f83-129
- Hatton, A. D. 2002. Influence of photochemistry on the marine biogeochemical cycle of dimethylsulphide in the northern North Sea. *Deep. Res. II* **49**: 3039–3052. doi:10.1016/S0967-0645(02)00070-X
- Hatton, A. D., L. Darroch, and G. Malin. 2004. The role of dimethylsulphoxide in the marine biogeochemical cycle of dimethylsulphide, p. 29–56. *In Oceanography and Marine Biology: An Annual Review.*
- Hatton, A. D., G. Malln, A. G. McEwan, and P. S. Liss. 1994. Determination of dimethylsulfoxide in aqueous solution by an enzyme-linked method. *Anal. Chem.* **66**: 4093–4096.

- Hatton, A. D., D. M. Shenoy, M. C. Hart, A. Mogg, and D. H. Green. 2012. Metabolism of DMSP, DMS and DMSO by the cultivable bacterial community associated with the DMSP-producing dinoflagellate *Scrippsiella trochoidea*. *Biogeochemistry* **110**: 131–146. doi:10.1007/s10533-012-9702-7
- Hatton, A. D., and S. T. Wilson. 2007. Particulate dimethylsulphoxide and dimethylsulphonioacetate in phytoplankton cultures and Scottish coastal waters. *Aquat. Sci.* **69**: 330–340. doi:10.1007/s00027-007-0891-4
- Herr, A. E., J. W. H. Dacey, R. P. Kiene, R. D. McCulloch, N. Schuback, and P. D. Tortell. 2020. Potential roles of dimethylsulfoxide in regional sulfur cycling and phytoplankton physiological ecology in the NE Subarctic Pacific. *Limnol. Oceanogr.* 1–19. doi:10.1002/lno.11589
- Herr, A. E., R. P. Kiene, J. W. H. Dacey, and P. D. Tortell. 2019. Patterns and drivers of dimethylsulfide concentration in the northeast subarctic Pacific across multiple spatial and temporal scales. *Biogeosciences* **16**: 1729–1754. doi:10.5194/bg-16-1729-2019
- Hickey, B. M., R. E. Thomson, H. Yih, and P. H. LeBlond. 1991. Velocity and temperature fluctuations in a buoyancy-driven current off Vancouver Island. *J. Geophys. Res.* **96**: 10507–10517. doi:10.1029/90JC02578
- Hobson, L. A., and M. R. McQuoid. 1997. Temporal variations among planktonic diatom assemblages in a turbulent environment of the southern Strait of Georgia, British Columbia, Canada. *Mar. Ecol. Prog. Ser.* **150**: 263–274. doi:10.3354/meps150263
- Ianson, D., S. E. Allen, S. L. Harris, K. J. Orians, D. E. Varela, and C. S. Wong. 2003. The inorganic carbon system in the coastal upwelling region west of Vancouver Island, Canada. *Deep Sea Res. Part I Oceanogr. Res. Pap.* **50**: 1023–1042. doi:10.1016/S0967-

0637(03)00114-6

- Jackson, J. M., R. E. Thomson, L. N. Brown, P. G. Willis, and G. A. Borstad. 2015. Satellite chlorophyll off the British Columbia Coast, 1997-2010. *J. Geophys. Res. Ocean.* **120**: 4709–4728. doi:10.1002/2014JC010496.
- Jarníková, T., J. Dacey, M. Lizotte, M. Levasseur, and P. Tortell. 2018. The distribution of methylated sulfur compounds, DMS and DMSP, in Canadian subarctic and Arctic marine waters during summer 2015. *Biogeosciences* **15**: 2449–2465. doi:10.5194/bg-15-2449-2018
- Keith Johnson, W., L. A. Miller, N. E. Sutherland, and C. S. Wong. 2005. Iron transport by mesoscale Haida eddies in the Gulf of Alaska. *Deep Sea Res. Part II Top. Stud. Oceanogr.* **52**: 933–953. doi:10.1016/J.DSR2.2004.08.017
- Kiene, R. P., and G. Gerard. 1994. Determination of trace levels of dimethylsulfoxide (DMSO) in seawater and rainwater. *Mar. Chem.* **47**: 1–12. doi:10.1016/0304-4203(94)90009-4
- Kiene, R. P., and L. J. Linn. 2000. The fate of dissolved dimethylsulfoniopropionate (DMSP) in seawater: Tracer studies using ^{35}S -DMSP. *Geochim. Cosmochim. Acta* **64**: 2797–2810. doi:10.1016/S0016-7037(00)00399-9
- Kiene, R. P., L. J. Linn, and J. A. Bruton. 2000. New and important roles for DMSP in marine microbial communities. *J. Sea Res.* **43**: 209–224. doi:10.1016/S1385-1101(00)00023-X
- Kinsey, J. D., and D. J. Kieber. 2016. Microwave preservation method for DMSP, DMSO, and acrylate in unfiltered seawater and phytoplankton culture samples. *Limnol. Oceanogr. Methods* **14**: 196–209. doi:10.1002/lom3.10081
- Korhonen, H., K. S. Carslaw, D. V. Spracklen, G. W. Mann, and M. T. Woodhouse. 2008. Influence of oceanic dimethyl sulfide emissions on cloud condensation nuclei concentrations and seasonality over the remote Southern Hemisphere oceans: A global

- model study. *J. Geophys. Res. Atmos.* **113**: 1–16. doi:10.1029/2007JD009718
- Lana, A., T. G. Bell, R. Simó, and others. 2011. An updated climatology of surface dimethylsulfide concentrations and emission fluxes in the global ocean. *Global Biogeochem. Cycles* **25**: GB1004. doi:10.1029/2010GB003850
- Lee, P. A., and S. J. de Mora. 1999. Intracellular dimethylsulfoxide (DMSO) in unicellular marine algae: speculations on its origin and possible biological role. *J. Phycol* **35**: 8–18. doi:10.1046/j.1529-8817.1999.3510008.x
- Li, C., G. P. Yang, D. J. Kieber, J. Motard-Côté, and R. P. Kiene. 2015. Assessment of DMSP turnover reveals a non-bioavailable pool of dissolved DMSP in coastal waters of the Gulf of Mexico. *Environ. Chem.* **13**: 266–279. doi:10.1071/EN15052
- Lidbury, I., E. Kröber, Z. Zhang, Y. Zhu, J. C. Murrell, Y. Chen, and H. Schäfer. 2016. A mechanism for bacterial transformation of dimethylsulfide to dimethylsulfoxide: a missing link in the marine organic sulfur cycle. *Environ. Microbiol.* **18**: 2754–2766. doi:10.1111/1462-2920.13354
- Lizotte, M., M. Levasseur, I. Kudo, K. Suzuki, A. Tsuda, R. P. Kiene, and M. G. Scarratt. 2009. Iron-induced alterations of bacterial DMSP metabolism in the western subarctic Pacific during SEEDS-II. *Deep. Res. Part II Top. Stud. Oceanogr.* **56**: 2889–2898. doi:10.1016/j.dsr2.2009.06.012
- Lovelock, J. E., R. Maggs, and R. Rasmussen. 1972. Atmospheric dimethyl sulfide and natural sulphur cycle. *Nature* **237**: 452–453. doi:10.1038/237452a0
- Masson, D., and A. Pena. 2009. Chlorophyll distribution in a temperate estuary : The Strait of Georgia and Juan de Fuca Strait. *Estuarine, Coast. Shelf Sci.* **82**: 19–28. doi:10.1016/j.ecss.2008.12.022

- McCulloch, R. D., A. Herr, J. Dacey, and P. D. Tortell. 2020. Application of purge and trap-atmospheric pressure chemical ionization-tandem mass spectrometry for the determination of dimethyl sulfide in seawater. *Limnol. Oceanogr. Methods* **18**: 547–559. doi:10.1002/lom3.10381
- Murphy, D. M., J. R. Anderson, P. K. Quinn, and others. 1998. Influence of sea-salt on aerosol radiative properties in the Southern Ocean marine boundary layer. *Nature* **392**: 62–65. doi:10.1038/32138
- Nelson, N. B., and D. A. Siegel. 2013. The global distribution and dynamics of chromophoric dissolved organic matter. *Ann. Rev. Mar. Sci.* **5**: 447–476. doi:10.1146/annurev-marine-120710-100751
- Nemcek, N., D. Ianson, and P. D. Tortell. 2008. A high-resolution survey of DMS, CO₂, and O₂/Ar distributions in productive coastal waters. *Global Biogeochem. Cycles* **22**: 1–13. doi:10.1029/2006GB002879
- Nishiguchi, M. K., and G. N. Somero. 1992. Temperature- and concentration-dependence of compatibility of the organic osmolyte β -dimethylsulfoniopropionate. *Cryobiology* **29**: 118–124. doi:10.1016/0011-2240(92)90011-P
- Peterson, T. D., D. W. Crawford, and P. J. Harrison. 2011. Evolution of the phytoplankton assemblage in a long-lived mesoscale eddy in the eastern Gulf of Alaska. *Mar. Ecol. Prog. Ser.* **424**: 53–73. doi:10.3354/meps08943
- Peterson, T. D., H. N. J. Toews, C. L. K. Robinson, and P. J. Harrison. 2007. Nutrient and phytoplankton dynamics in the Queen Charlotte Islands (Canada) during the summer upwelling seasons of 2001-2002. *J. Plankton Res.* **29**: 219–239. doi:10.1093/plankt/fbm010
- Quinn, P. K., and T. S. Bates. 2011. The case against climate regulation via oceanic

- phytoplankton sulphur emissions. *Nature* **480**: 51–56. doi:10.1038/nature10580
- Royer, S. J., M. Levasseur, M. Lizotte, and others. 2010. Microbial dimethylsulfoniopropionate (DMSP) dynamics along a natural iron gradient in the northeast subarctic Pacific. *Limnol. Oceanogr.* **55**: 1614–1626. doi:10.4319/lo.2010.55.4.1614
- Sharma, S., R. Vingarzan, L. A. Barrie, A. Norman, A. Sirois, M. Henry, and C. DiCenzo. 2003. Concentrations of dimethyl sulfide in the Strait of Georgia and its impact on the atmospheric sulfur budget of the Canadian West Coast. *J. Geophys. Res. Atmos.* **108**: 1–17. doi:10.1029/2002jd002447
- Sherry, N. D., P. W. Boyd, K. Sugimoto, and P. J. Harrison. 1999. Seasonal and spatial patterns of heterotrophic bacterial production, respiration, and biomass in the subarctic NE Pacific. *Deep. Res. Part II Top. Stud. Oceanogr.* **46**: 2557–2578. doi:10.1016/S0967-0645(99)00076-4
- Simó, R. 2001. Production of atmospheric sulfur by oceanic plankton: biogeochemical, ecological and evolutionary links. *Trends Ecol. Evol.* **16**: 287–294. doi:10.1016/S0169-5347(01)02152-8
- Simó, R., C. Pedros-Alio, G. Malin, and J. O. Grimalt. 2000. Biological turnover of DMS, DMSP and DMSO in contrasting open-sea waters. *Mar. Ecol. Prog. Ser.* **203**: 1–11. doi:10.3354/meps203001
- Speeckaert, G., A. V. Borges, W. Champenois, C. Royer, and N. Gypens. 2018. Annual cycle of dimethylsulfoniopropionate (DMSP) and dimethylsulfoxide (DMSO) related to phytoplankton succession in the Southern North Sea. *Sci. Total Environ.* **622–623**: 362–372. doi:10.1016/j.scitotenv.2017.11.359
- Speeckaert, G., A. V. Borges, and N. Gypens. 2019. Salinity and growth effects on

- dimethylsulfoniopropionate (DMSP) and dimethylsulfoxide (DMSO) cell quotas of *Skeletonema costatum*, *Phaeocystis globosa* and *Heterocapsa triquetra*. *Estuar. Coast. Shelf Sci.* **226**: 106275. doi:10.1016/j.ecss.2019.106275
- Spiese, C. E., D. J. Kieber, C. T. Nomura, and R. P. Kiene. 2009. Reduction of dimethylsulfoxide to dimethylsulfide by marine phytoplankton. *Limnol. Oceanogr.* **54**: 560–570. doi:10.4319/lo.2009.54.2.0560
- Spiese, C. E., and E. A. Tatarkov. 2014. Dimethylsulfoxide reduction activity is linked to nutrient stress in *Thalassiosira pseudonana* NCMA 1335. *Mar. Ecol. Prog. Ser.* **507**: 31–38. doi:10.3354/meps10842
- Stefels, J. 2000. Physiological aspects of the production and conversion of DMSP in marine algae and higher plants. *J. Sea Res.* **43**: 183–197. doi:10.1016/S1385-1101(00)00030-7
- Stefels, J., M. Steinke, S. Turner, G. Malin, and S. Belviso. 2007. Environmental constraints on the production and removal of the climatically active gas dimethylsulphide (DMS) and implications for ecosystem modelling. *Biogeochemistry* **83**: 245–275. doi:10.1007/s10533-007-9091-5
- Stockner, J. G., D. D. Cliff, and K. R. S. Shortreed. 1979. Phytoplankton Ecology of the Strait of Georgia, British Columbia. *J. Fish. Res. Board Canada* **36**: 657–666. doi:10.1139/f79-095
- Sunda, W., D. J. Kieber, R. P. Kiene, and S. Huntsman. 2002. An antioxidant function for DMSP and DMS in marine algae. *Nature* **418**: 317–320. doi:10.1038/nature00851
- Sweeney, C., E. Gloor, A. R. Jacobson, R. M. Key, G. McKinley, J. L. Sarmiento, and R. Wanninkhof. 2007. Constraining global air-sea gas exchange for CO₂ with recent bomb ¹⁴C measurements. *Global Biogeochem. Cycles* **21**: GB2015. doi:10.1029/2006GB002784
- Taalba, A., H. Xie, M. G. Scarratt, S. Bélanger, and M. Levasseur. 2013. Photooxidation of

- dimethylsulfide (DMS) in the Canadian Arctic. *Biogeosciences* **10**: 6793–6806.
doi:10.5194/bg-10-6793-2013
- Tanaka, J. Y., J. R. Walsh, K. R. Diller, J. J. Brand, and S. J. Aggarwal. 2001. Algae permeability to Me₂SO from -3 to 23degC. *Cryobiology* **42**: 286–300.
doi:10.1006/cryo.2001.2334
- Thomson, R. E. 1981. *Oceanography of the British Columbia Coast*, Department of Fisheries and Oceans.
- Thume, K., B. Gebser, L. Chen, N. Meyer, D. J. Kieber, and G. Pohnert. 2018. The metabolite dimethylsulfoxonium propionate extends the marine organosulfur cycle. *Nature* **563**: 412–415. doi:10.1038/s41586-018-0675-0
- Tortell, P. D., A. Merzouk, D. Ianson, R. Pawlowicz, and D. R. Yelland. 2012. Influence of regional climate forcing on surface water pCO₂, ΔO₂/Ar and dimethylsulfide (DMS) along the southern British Columbia coast. *Cont. Shelf Res.* **47**: 119–132.
doi:10.1016/j.csr.2012.07.007
- Tripp, H. J., J. B. Kitner, M. S. Schwalbach, J. W. H. Dacey, L. J. Wilhelm, and S. J. Giovannoni. 2008. SAR11 marine bacteria require exogenous reduced sulphur for growth. *Nature* **452**: 741–744. doi:10.1038/nature06776
- Tyssebotn, I. M. B., J. D. Kinsey, D. J. Kieber, R. P. Kiene, A. N. Rellinger, and J. Motard-Côté. 2017. Concentrations, biological uptake, and respiration of dissolved acrylate and dimethylsulfoxide in the northern Gulf of Mexico. *Limnol. Oceanogr.* **62**: 1198–1218.
doi:10.1002/lno.10495
- Uher, G., J. J. Pillans, A. D. Hatton, and R. C. Upstill-Goddard. 2017. Photochemical oxidation of dimethylsulphide to dimethylsulphoxide in estuarine and coastal waters. *Chemosphere*

- 186**: 805–816. doi:10.1016/j.chemosphere.2017.08.050
- del Valle, D. A., D. J. Kieber, and R. P. Kiene. 2007. Depth-dependent fate of biologically-consumed dimethylsulfide in the Sargasso Sea. *Mar. Chem.* **103**: 197–208.
doi:10.1016/j.marchem.2006.07.005
- del Valle, D. A., D. J. Kieber, D. A. Toole, J. Bisgrove, and R. P. Kiene. 2009. Dissolved DMSO production via biological and photochemical oxidation of dissolved DMS in the Ross Sea, Antarctica. *Deep. Res. Part I Oceanogr. Res. Pap.* **56**: 166–177.
doi:10.1016/j.dsr.2008.09.005
- del Valle, D. A., D. Slezak, C. M. Smith, A. N. Rellinger, D. J. Kieber, and R. P. Kiene. 2011. Effect of acidification on preservation of DMSP in seawater and phytoplankton cultures: Evidence for rapid loss and cleavage of DMSP in samples containing *Phaeocystis* sp. *Mar. Chem.* **124**: 57–67. doi:10.1016/j.marchem.2010.12.002
- Vallina, S. M., R. Simó, and M. Manizza. 2007. Weak response of oceanic dimethylsulfide to upper mixing shoaling induced by global warming. *Proc. Natl. Acad. Sci. U. S. A.* **104**: 16004–16009. doi:10.1073/pnas.0700843104
- Vila-Costa, M., R. Simó, H. Harada, J. M. Gasol, D. Slezak, and R. P. Kiene. 2006a. Dimethylsulfoniopropionate uptake by marine phytoplankton. *Science (80-.)*. **314**: 652–654. doi:10.1126/science.1131043
- Vila-Costa, M., D. A. Del Valle, J. M. González, D. Slezak, R. P. Kiene, O. Sánchez, and R. Simó. 2006b. Phylogenetic identification and metabolism of marine dimethylsulfide-consuming bacteria. *Environ. Microbiol.* **8**: 2189–2200. doi:10.1111/j.1462-2920.2006.01102.x
- Whitney, F. A., W. R. Crawford, and P. J. Harrison. 2005. Physical processes that enhance

- nutrient transport and primary productivity in the coastal and open ocean of the subarctic NE Pacific. *Deep. Res. II* **52**: 681–706. doi:10.1016/j.dsr2.2004.12.023
- Whitney, F., and M. Robert. 2002. Structure of Haida Eddies and their transport of nutrient from coastal margins into the NE Pacific Ocean. *J. Oceanogr.* **58**: 715–723.
doi:10.1023/A:1022850508403
- Williams, B. T., K. Cowles, A. Bermejo Martínez, and others. 2019. Bacteria are important dimethylsulfoniopropionate producers in coastal sediments. *Nat. Microbiol.* **4**: 1815–1825.
doi:10.1038/s41564-019-0527-1
- Wittek, B., G. Carnat, J. L. Tison, and N. Gypens. 2020. Response of dimethylsulfoniopropionate (DMSP) and dimethylsulfoxide (DMSO) cell quotas to salinity and temperature shifts in the sea-ice diatom *Fragilariopsis cylindrus*. *Polar Biol.* **43**: 483–494. doi:10.1007/s00300-020-02651-0
- Yang, G., C. Li, J. Qi, L. Hu, and H. Hou. 2007. Photochemical oxidation of dimethylsulfide in seawater. *Acta Oceanol. Sin.* **26**: 34–42.
- Yoch, D. C., J. H. Ansele, and K. S. Rabinowitz. 1997. Evidence for intracellular and extracellular dimethylsulfoniopropionate (DMSP) lyases and DMSP uptake sites in two species of marine bacteria. *Appl. Environ. Microbiol.* **63**: 3182–3188.
doi:10.1128/aem.63.8.3182-3188.1997
- Zapata, M., F. Rodríguez, and J. L. Garrido. 2000. Separation of chlorophylls and carotenoids from marine phytoplankton: A new HPLC method using a reversed phase C8 column and pyridine-containing mobile phases. *Mar. Ecol. Prog. Ser.* **195**: 29–45.
doi:10.3354/meps195029
- Zheng, Y., J. Wang, S. Zhou, and others. 2020. Bacteria are important

dimethylsulfoniopropionate producers in marine aphotic and high-pressure environments.

Nat. Commun. **11**: 4658. doi:10.1038/s41467-020-18434-4

Zhou, L., M. Wang, H. Zhang, G. Yang, Z. Limin, W. Min, Z. Honghai, and Y. Guipeng. 2020.

Seasonal and spatial variations of dimethylsulfoxide (DMSO) in the East China Sea and the

Yellow Sea. Acta Oceanol. Sin. **39**: 1–11. doi:10.1007/s13131-020-1549-5

Zindler, C., A. Bracher, C. A. Marandino, B. Taylor, E. Torrecilla, A. Kock, and H. W. Bange.

2013. Sulphur compounds, methane, and phytoplankton: Interactions along a north-south

transit in the western Pacific Ocean. Biogeosciences **10**: 3297–3311. doi:10.5194/bg-10-

3297-2013

Appendices

The appendices below describe several laboratory tests I have performed for method optimization (Appendices A and B). Appendix C presents supplementary materials for the main body of this thesis.

Appendix A DMSP preservation

In preparation for a sampling cruise in September, 2019, a series of DMSP preservation tests were conducted to examine the most suitable preservation method for unfiltered DMSP seawater samples. The most common preservation method of DMSP is acidification (Curran et al. 1998). However, del Valle et al. (2011) suggested a substantial loss of DMSP in the colonial *Phaeocystis* seawater samples by acid preservation, which was not detected in other waters with minor *Phaeocystis* components. Since *Phaeocystis* is not abundant in the coastal waters around Vancouver Island (Harrison et al. 1983; Hobson and McQuoid 1997; Harris et al. 2009), I compared the conventional acidification method with the microwave method suggested by Kinsey and Kieber (2016), and optimized the amount of acid used for preservation to reduce hazardous waste. Seawater samples were collected at Wreck Beach and Kitslano Beach, Vancouver. Preserved and controlled samples were analyzed in the laboratory upon sample collection at T0 (day 0), and analyzed over the course of storage to compare the concentration change.

Results from these experiments show that both acidification and microwave methods successfully preserve DMSP samples for at least 1-2 weeks. Results also suggest that addition of 100 μL of 50% H_2SO_4 per every ~ 10 mL seawater sample is sufficient for preservation purpose. Since microwaving DMSP samples onboard is time-consuming and difficult to perform, we

adopted the acidification method. This method is also adopted in the following Saanich sampling cruises and other DMSP samples. The sub-appendices below show raw results and notes from three DMSP preservation experiments. Statistical tests were used to compare the means of non-normally distributed groups, and an α -value of 0.05 was used as a measure of statistical significance.

A.1 Optimal amount of acid used for preservation

Replicates of small volume seawater samples ($n = 5$; volume ~ 10 mL) were collected on May 16, 2019 at Wreck Beach, Vancouver. Samples were preserved with addition of 100 μ L, 200 μ L and 300 μ L of 50% H_2SO_4 , and stored in the dark at a 4°C fridge for 4 weeks. Due to experimental problems, concentrations of unpreserved DMSP samples at T0 were missing, and thus the concentration change between T0 and the last time point cannot be compared. However, pH of the DMSP samples acidified by various amounts of H_2SO_4 was measured, and it remained <1 throughout the storage period for all acidified samples. A Mann-Whitney U test was done to compare the concentration means of three non-parametric groups (100 μ L, 200 μ L and 300 μ L) after 4 weeks of storage. There was no statistical difference among the three treatments ($p = 0.934$). Therefore, acidification using 100 μ L of 50% H_2SO_4 per 10 mL seawater is adopted for DMSP acidification to minimize hazardous waste.

A.2 Acidification method

Triplicates of small volume seawater samples (volume ~ 10 mL) were collected on May 23, 2019 at Kitslano Beach, Vancouver. Samples were preserved with addition of 100 μ L of 50% H_2SO_4 , and stored in the dark at a 4°C fridge. Results show that when analyzed immediately upon

sample collection, a pre-sparge step for removal of endogenous DMS is necessary. A Mann-Whitney Test (SPSS Software Inc.) was performed to evaluate statistical difference between the means of two non-parametric groups. Statistical results show that there is no significant difference between acidified samples with and without pre-sparge ($p = 0.513$). No statistical difference was also found between the untreated T0 and acidified T3 without pre-sparge step ($p = 0.513$). Therefore, it is suggested that a pre-sparge step prior to sample analysis is not necessary after two weeks of storage time.

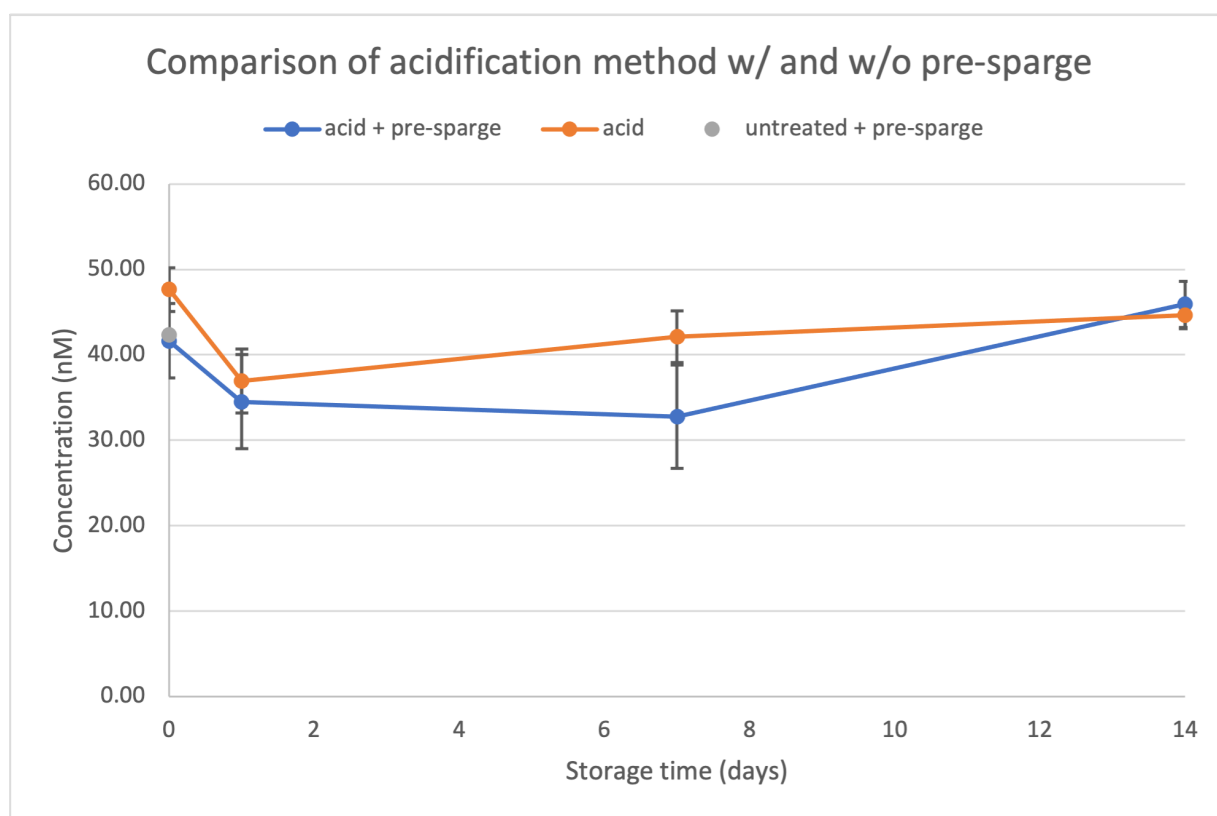


Figure A.2.1 Comparison of acidification method with and without pre-sparge. Error bars represent standard deviations.

A.3 Microwave method

Replicates of small volume seawater samples ($n = 5$; volume ~ 10 mL) were collected on June 4, 2019 at Kitslano Beach, Vancouver. Following the preservation method described in Kinsey and Kieber (2016), samples were preserved by microwaving them to boiling, cooled down to room temperature, and stored in the dark at a 4°C fridge. Similar to the acidification method, after several days of storage, a pre-sparge step prior to DMSP analysis to remove endogenous DMS is unnecessary as there is no statistical difference between the two groups at day 7 ($p = 0.917$). No statistical difference was also found between the untreated T0 and microwaved T3 without pre-sparge step ($p = 0.251$).

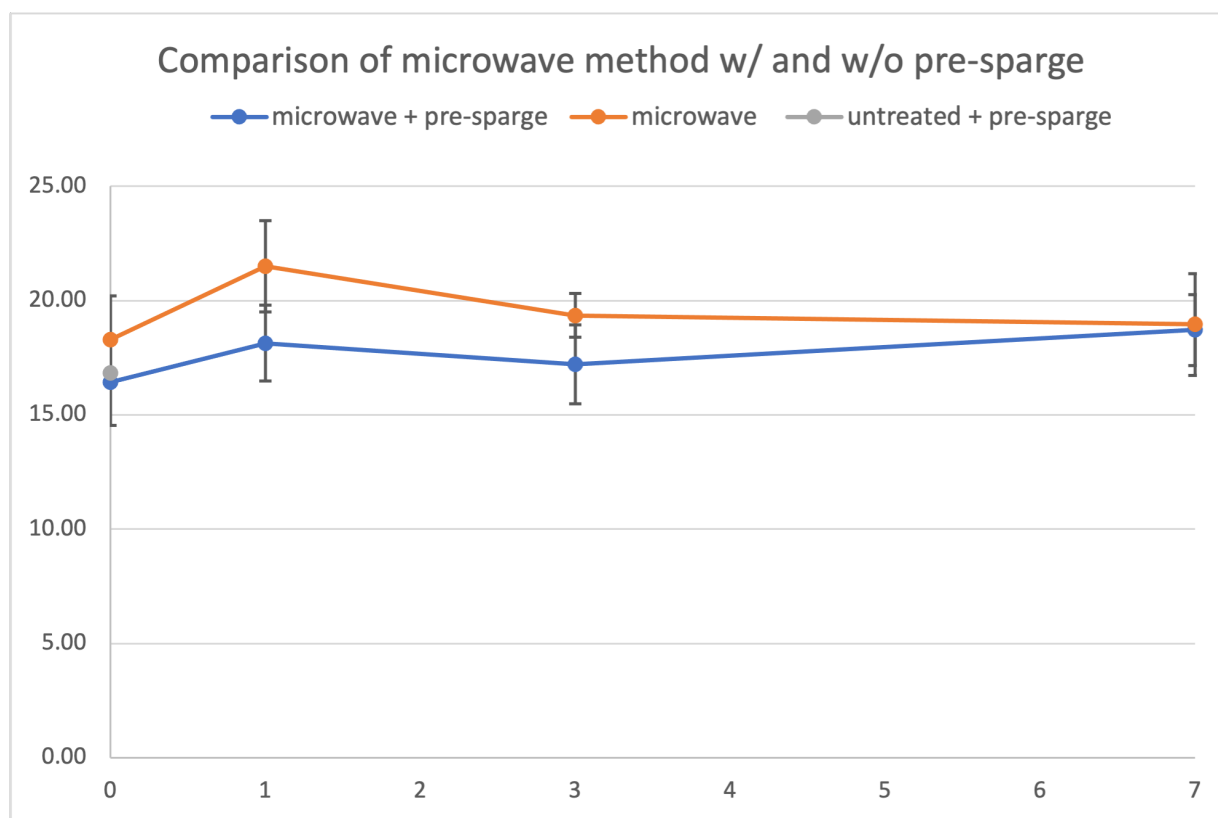


Figure A.3.1 Comparison of microwave method with and without pre-sparge. Error bars represent standard deviations.

Appendix B Protocol of DMSO analysis by TiCl_3

Due to deficiency of DMSO reductase for the DMSO reduction method, we adopted the TiCl_3 reduction method described in Kiene and Gerard (1994) to analyze the discrete unfiltered DMSO samples collected during the 2019 La Perouse cruise. Below is a detailed protocol of TiCl_3 reduction adopted from Kiene and Gerard (1994) and Deschaseaux et al. (2014).

B.1 Preparation of glassware prior to analysis

Prepare 10% HCl in fume hood at least one day prior to analysis. In the fume hood, slowly add 216 mL of 37% w/w HCl into ~800mL of Milli Q water using a glass funnel. Place the 10% HCl on a stir plate overnight.

Soak the glassware with 10% HCl for at least an hour to remove any dissolved DMSO or DMS in the glass, then rinse with Milli Q water. Bake the glassware at $>100^\circ\text{C}$ for at least an hour. When baking is done, cover the hot glassware with aluminum foil and leave them in the fume hood until it is cooled to room temperature.

While the glassware is in oven, turn on water bath and set temperature to 50°C , and thaw DMSO samples at room temperature in the dark. Sparge a small amount of TiCl_3 solution needed for analysis with N_2 for **at least** an hour. Note that sufficient sparging of TiCl_3 is particularly important to remove any endogenous DMS in the solution and minimize blanks. If possible, sparge TiCl_3 for two hours before use. An additional step can also be done to check if sparging is sufficient. Add 5 mL of Milli Q and 1 mL of TiCl_3 , and analyze the sample for DMS concentrations. If DMS is detectable in the sample, a longer period of sparging is needed. When the reagents are clean, prepare a 10 nM DMSO standard solution for calibration.

B.2 Experimental procedures of DMSO reduction by TiCl_3

After DMSO samples are thawed to room temperature, sparge them with N_2 to remove any endogenous DMS in the samples. To prepare blanks, add 5 mL of Milli Q water and 1 mL of TiCl_3 . For DMSO samples, add 5 mL of pre-sparged seawater samples or DMSO standard and 1 mL of TiCl_3 . Seal the vials with aluminum cap and gently mix the vials. Put them in water bath at 50 °C for one hour.

An hour later, remove the samples from water bath and cool to room temperature. Analyze the samples for DMS (see methods in Chapter 2). In our method, it is not necessary to make the samples basic prior to analysis, as previously suggested by Kiene and Gerard (1994). When the analysis is complete, dispose the Ti-contaminated waste in a designated container in the fume hood.

Appendix C Supplementary materials for Chapter 2

Below are supplementary figures, tables, and notes used in Chapter 2.

C.1 Calculation of turnover rate constants for net DMS production from DMSP cleavage and DMSO reduction

For the first-order reaction of DMSP cleavage:



Reaction rate is defined as:

$$rate = -\frac{d[DMSP]}{dt} = \frac{d[DMS]}{dt} = k_1[DMSP]$$

where k_1 is the rate constant for DMSP consumption (sum of all DMSP consumption pathways including assimilation to particulate, demethiolation/demethylation pathway and DMSP cleavage).

Therefore, k_1 can be derived by the change of natural logarithm of DMSP concentrations over time:

$$\ln[DMSP]_t - \ln[DMSP]_0 = -k_1 t$$

or,

$$\frac{\ln[DMSP]_t - \ln[DMSP]_0}{t} = -k_1$$

where $[DMSP]_t$ and $[DMSP]_0$ are DMSP concentrations at time t and $t = 0$.

Similarly, rate constant for net DMS production from DMSP cleavage (k_2) can be derived by:

$$\ln\{[DMSP]_0 - ([DMS]_t - [DMS]_0)\} - \ln[DMSP]_0 = -k_2 t$$

or,

$$\frac{\ln\{[DMSP]_0 - ([DMS]_t - [DMS]_0)\} - \ln[DMSP]_0}{t} = -k_2$$

where $[DMS]_t$ and $[DMS]_0$ are DMS concentration produced from DMSP cleavage at time t and t = 0. The rate constant calculated in this way represents DMSP change due to DMS production from DMSP cleavage, and the resulting DMS may be consumed simultaneously, thus it represents net DMS production from DMSP cleavage.

Therefore, for the stope isotope tracer experiments, rate constant for net DMS production from DMSP cleavage can be obtained from:

$$\frac{\ln([D_6 - DMSP]_0 - \Delta[D_6 - DMS]_t) - \ln[D_6 - DMSP]_0}{t} = -k_{DMSPcleav}$$

where $[D_6 - DMSP]_0$ is the starting concentration of tracer D₆-DMSP, and $\Delta[D_6 - DMS]_t$ is the concentration change of D₆-DMS between t and t = 0.

Similarly, rate constant for net DMS production from DMSO reduction can be obtained from:

$$\frac{\ln([D_6 - 13C_2 - DMSO]_0 - \Delta[D_6 - 3C_2 - DMS]_t) - \ln[D_6 - 3C_2 - DMSO]_0}{t} = -k_{DMSOred}$$

where $[D_6 - 13C_2 - DMSO]_0$ is the starting concentration of tracer $D_6-^{13}C_2$ -DMSO, and $\Delta[D_6 - 13C_2 - DMS]_t$ is the concentration change of $D_6-^{13}C_2$ -DMS between t and $t = 0$.

C.2 Statistical assessment of turnover rate constants

Isotope tracer experiments were conducted in triplicate incubation bags, with turnover rate constants for tracers in each bag computed individually, and averaged to obtain a mean value. Following Asher et al. (2017a; b) and Herr et al. (2020), tracer time-course data with $r^2 > 0.5$ were considered to represent statistically-significant linear regressions, while data with $r^2 < 0.04$ were considered to have rate constants below detection limit (or no net change as a result of various competing pathways). For those experiments with $0.04 < r^2 < 0.5$, Cook's Distance was computed to detect potential outliers and estimate the influence of individual data points on the linear regression. From this analysis, we removed the one point with greatest Cook's Distance to improve the correlation coefficients (r). The tracer dataset was considered unusable if the removal of this outlier did not improve the correlation coefficient (r^2 still below 0.5). Otherwise, turnover rate constants were re-calculated after removing the outlier point. Fig. C2.1 illustrates an example of this approach.

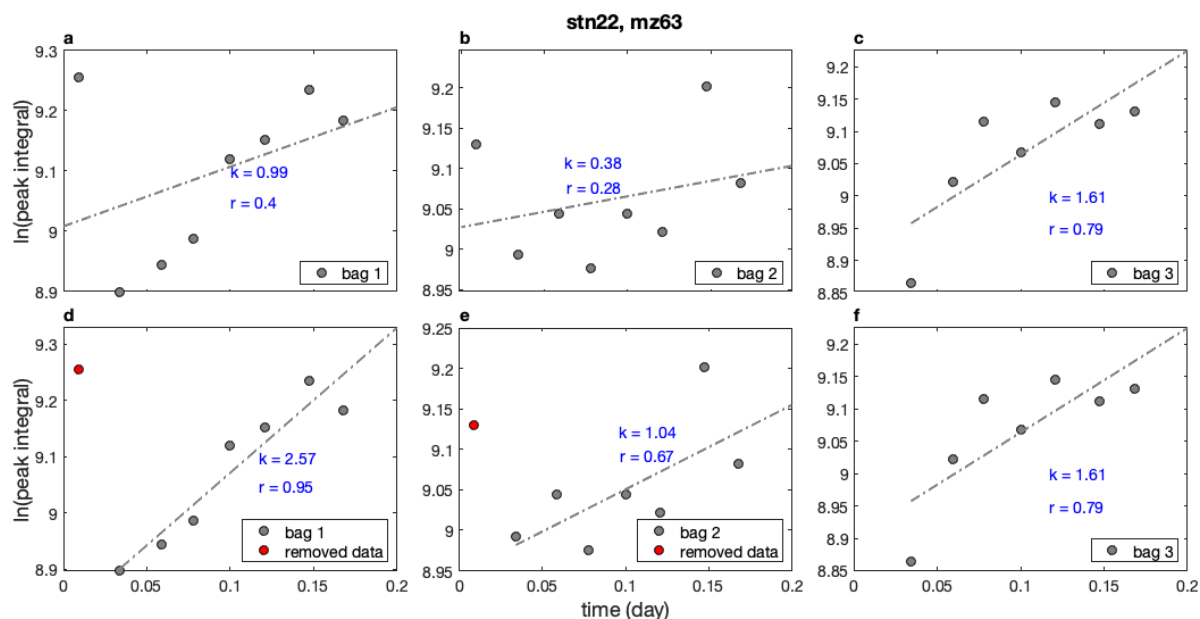


Figure C.2.1 Example of outlier removal based on the determination of the Cook's Distance metric. Panels (a-c) show the raw data of natural DMS evolution ($m/z = 63$) over the course of incubation at station 12. Bag 1 shows a high initial data point for the measured sample (T_0), which results in a low r value. Bag 2 has the lowest r value ($r = 0.28$, $r^2 = 0.056$) and a slope close to zero. Bag 3 has $r^2 > 0.5$ so the rate constant derived from this bag is accepted. Panels (d-f) illustrate the influence of removing one outlier on the slopes and correlation coefficients. After removing the first data point from bag 1 (panel d), the r value is significantly improved, and the revised rate constant derived from this bag is used. For bag 2, removing the outlier point with the greatest Cook's distance does not improve the r^2 value to reach the threshold ($r^2 = 0.5$), so the rate constant derived from bag 2 is not used in our analysis. Averaging slopes from bag 1 and 3 yields a mean rate constant of $2.09 \pm 0.68 \text{ d}^{-1}$ for net DMS change at station 22.

C.3 Supplementary figures for discussion

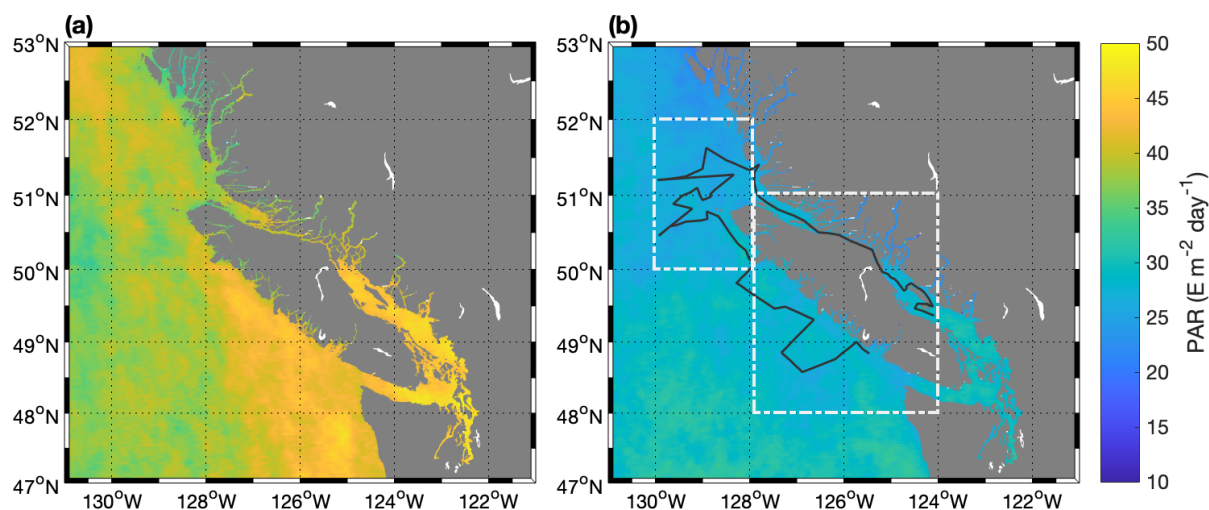


Figure C.3.1 Monthly-average distribution of photosynthetically active radiation (PAR) derived from the MODIS-Aqua satellite product with 4 km resolution in **(a)**: May 2017; **(b)**: September 2019. Black lines are cruise track in the 2019 September cruise. White dotted boxes indicate selected areas for estimating average PAR. The difference between the two years results from greater cloud cover in 2019, and the lower PAR levels may have acted to decrease DMS photo-oxidation rates.

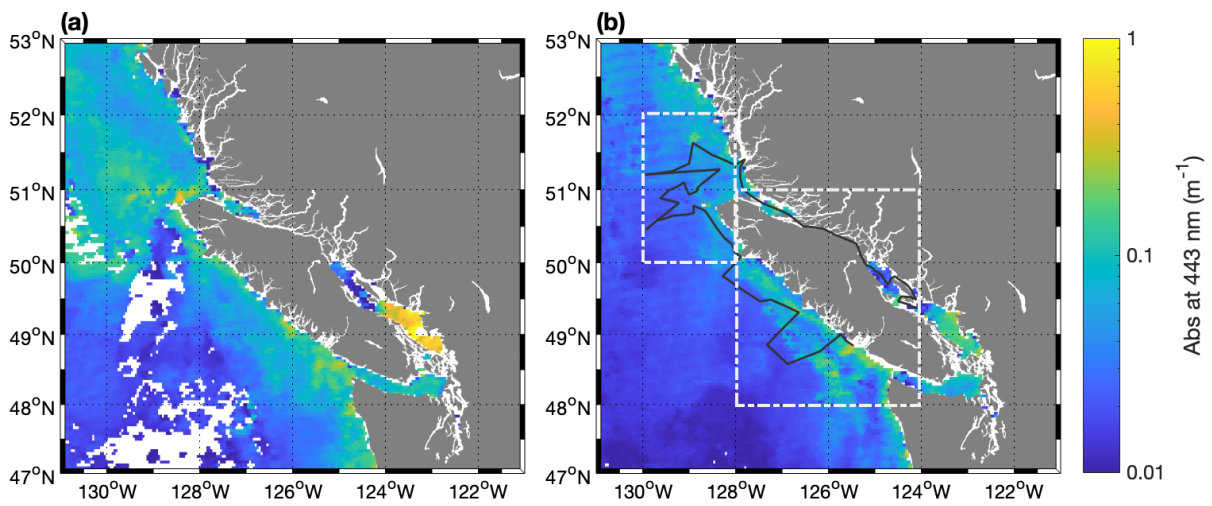


Figure C.3.2 Monthly-average distribution of absorbance due to gelbstof and detritus at 443 nm derived from the MODIS-Aqua satellite product with 4 km resolution in **(a)**: May 2017; **(b)**: September 2019. Black lines are cruise track in the 2019 September cruise. White dotted boxes indicate selected areas for estimating average PAR. The average absorbance in May, 2017 is 0.067 m⁻¹ and average absorbance in September, 2019 is 0.036 m⁻¹.

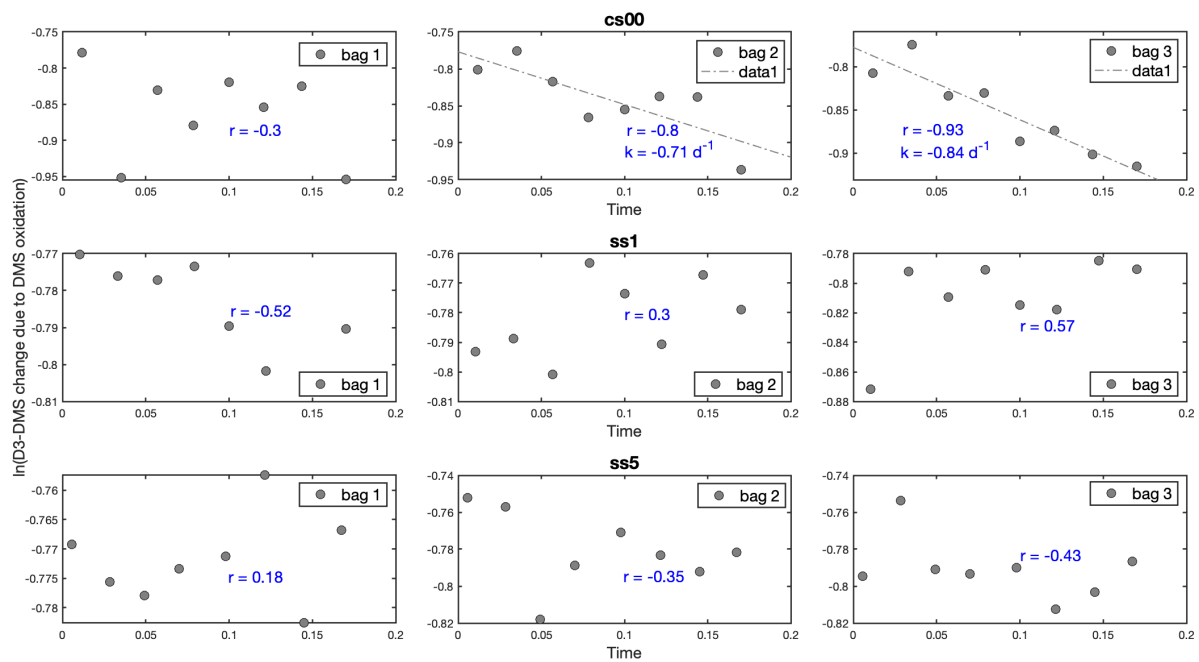


Figure C.3.3 Raw data of turnover rate measurements of DMS oxidation from station CS00, SS1 and SS5. Measurements represent the disappearance of D3-DMS due to DMS oxidation to DMSO.